Computer Assisted Mechanics and Engineering Sciences, 11: 167–195, 2004.

Artificial relations between quantities at nearest nodes or cells and the Newton iteration procedure for the modified pressure correction method

Shamil F. Araslanov
Research Institute of Mathematics and Mechanics, Kazan State University
17 Universitetskaya St, 420008 Kazan, Tatarstan, Russia

(Received December 13, 2002)

In this article a method for calculation of the finite-difference Navier–Stokes equations with a time step $\Delta t = h/u_{\text{flow}}$ (h is the average cell's size, u_{flow} flow velocity) at the minimal expenses of computer time is suggested.

To realize the Newton-type iteration scheme and in order to avoid solving large-volume linear systems of equations for points k, which contain the variations of unknowns not only at the point k but also at points k' neighbouring with the point k, we replace the unknown relations between the variations of quantities at nearest points k and k' with artificial ones. Therefore the unknowns at the point k can be directly determined via equations at the point k and one does not need to apply complicated technique. The introduction of artificial relations between the variations of quantities at nearest nodes or cells and the use of approximate equality $\mathbf{c}' \approx -\mathbf{c}$ relating geometric coefficients of both displaced and usual cells make it possible to obtain formulas for correct rates of change of the residuals of the equations. Consequently, only four global iterations and 4 to 5 (in average) inner pressure correction iterations for every global iteration suffice to provide the convergence.

Keywords: heat transfer flows, approximation technique, Newton iteration method, pressure correction

1. Introduction

The Newton procedure can diverge if the initial guesses differ significantly from the target values. If these initial guesses are taken for the time $t + \Delta t$ as the values known for the time t, and the time step Δt is chosen with the requirement to provide convergence within an approximately given number of iterations, then the divergence will be avoided due to such a restriction of the time step. To use a time step which were as large as possible, it is important to possess correct rates of the change of residuals (**CRCR**). We suggest a method for obtaining formulas of CRCR for solving the discretized Navier–Stokes equations with the Newton iteration procedure. We discretize the Navier–Stokes equations by using a weighted scheme with the weight ω. To realize the Newton-type iteration scheme and in order to avoid solving large linear systems of equations for cells j or for nodes i, which contain the unknowns δp, $\delta\rho$, δI not only at the cell j but also at the cells j' neighbouring with the cell j or contain the unknowns $\delta\mathbf{u}$ not only at the node i but also at the nodes i' neighbouring with the node i, we replace the unknown relations between the variations of quantities at nearest cells j and j' or nodes i and i' by artificial ones. The introduction of artificial relations between the variations of quantities at nearest nodes or cells and the use of approximate equality $\mathbf{c}' \approx -\mathbf{c}$ relating geometric coefficients of both displaced and usual cells make it possible to obtain formulas for CRCR.

In compressible flows, the Navier–Stokes equations yield a pressure correction equation which is the wave equation. Traditionally, to discharge the CFL-condition, the pressure correction equation has to be solved. If one does not solve the pressure correction equation, then the time step is bounded by the value h/a (here a is the sound speed, h the average cell's size) for single iteration, by $2h/a$ for two iterations, etc. Some test problems with a low Mach number flow (without pressure

correction procedure), gave us Δt bounded by $2h/a$ within 2 iterations and $\omega = 0.6$. If we take a larger time step, then the computation time increases proportionally due to an increase of the number of iterations.

All known pressure correction methods are usually reduced to solving the pressure correction equation containing both a discretized Laplace operator of pressure and some other terms. This equation has usually to be solved over the whole computation domain. Some effective methods are known, e.g. those based on the tridiagonal matrix algorithm; however, they require large computation time. Moreover, some terms and coefficients should be refined within iterations, which also increases computation costs. Next, the ordinary discretized equations for density and momentum are equipped with some comprehensible boundary values of pressure, density, and velocity. However, the pressure correction equation requires additional boundary values of the pressure. To determine these values, various complicated methods should be used; these methods depend on the nature of flows, computation domains, and mesh shapes (see [1]).

The above reasons yielded an intrinsic intent to avoid the usage of the pressure correction equation in computations. The only aim we apply this equation is to obtain the CRCR formula $\partial \mathrm{Q}_\rho / \partial p$. In the computation we use the ordinary discretized equations for both the density ρ and momentum $\rho\mathbf{u}$. By the Newton inner iterations we call the iterations carried out for these equations. The internal energy I, density, and velocity are determined within the global iterations of the Newton method with the use of CRCR. Thus organized, these Newton inner and global iterations brought us a notable result: the time step Δt reaches the value h/u_{flow} within 4 global iterations (each of them with about 4 to 5 inner iterations). The computation time required for a single time step is approx. 6 times greater than in case of an explicit scheme without pressure correction. Clearly, SIMPLE-type procedures require greater computation time and therefore are less efficient. In addition, in contrast to [2], now, for the numerical computation of an unsteady flow, we do not need to use a scaling transformation (see [3]). Compared with the suggested method, the scaling transformation has a limited adaptability, because it can be applied only to flows with low Mach number and results in errors in determination of both frequency and amplitude of acoustic oscillations. Within our procedure Δt turns to be lesser than h/u_{flow} if the boundary quantities vary quickly with time. If they change slowly, Δt attains the value h/u_{flow}.

Here, instead of hexahedral cells in [2], we apply arbitrary polyhedral cells. A fragment of such a mesh is shown in Fig. 1. In what follows the so-called staggered arrangement is used (see [4]): the values of the density ρ, the internal energy I, and the pressure p are assigned to the centroids of cells j, while the speed $\mathbf{u}$ (with components u, v, w) and the x, y, z coordinates are related to the nodes i which are the vertices of the polyhedral cells. Their centroids are vertices of, say, "good displaced polyhedral cells" (see [2]).

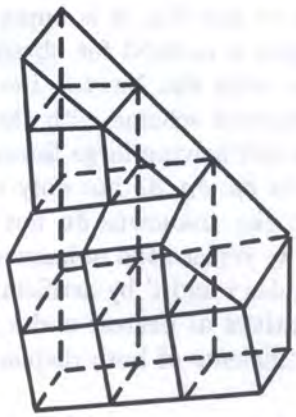

Fig. 1. A fragment of the mesh

As we have noted above, we replace unknown relations between the quantities at nearest nodes or cells with the artificial ones. Thus, in these formulas, the following parameters arise: ω_{p0}, ω_{u0},

ω_{I0}, $\omega_{\rho u0}$, $\omega_{\rho uu0}$. They express the artificially given relations between the variations of quantities indicated in the subscripts (for example, $\delta\rho\mathbf{u}_{j'} \approx \omega_{\rho u0}\delta\rho\mathbf{u}_j$). As soon as the formulas for CRCR have been deduced, one can arrange these parameters in such a way that a divergence will be prevented. For example, in our computation, we take the parameters ω_{p0}, ω_{u0}, ω_{I0}, $\omega_{\rho u0}$, $\omega_{\rho uu0}$ equal to -1. This way is similar to that in [2], where we had $\omega_{p0} = -1$; in the same paper the quantity ω_{p0} was treated as the derivative of pressure in the adjacent cell j' with respect to the pressure in the cell j under consideration. Here, in obtaining the formulas of CRCR, one can suppose that the central difference scheme for approximation of spatial operators are used; however, this is not valid completely. To explain this, consider an example in the one-dimensional case. For the inner pressure correction iteration, the following approximation is obtained for the variation of the residual of the mass conservation equation at the cell j:

$$\delta\mathrm{Q}_{\rho j} \approx \delta\,\partial\rho_j/\partial t - \omega^2\Delta t\delta\,\mathrm{div}\,(\mathrm{grad}\,p)_j \approx \left[\frac{\partial\rho}{\partial p}\frac{1}{\Delta t} + (1-\omega_{p0})\omega^2\Delta t\frac{2}{h^2}\right]\delta p_j\,.$$

Obviously, this formula fails to correspond to any difference approximation of spatial operators, because here no variations $\delta p_{j'}$ are present. Note that, in order to approximate the spatial operators, concrete difference schemes are used only for calculation of the residuals but not their CRCR. However, by our opinion, for the Newton iteration procedures the obtained formulas of CRCR may be appropriate for various difference schemes of approximation of the residuals.

Earlier, in obtaining a formula of the rate of change of residual for a certain equation with the unknown q, some authors should neglect q at points adjacent to the point under consideration. To avoid the divergence, they usually took the relaxation parameter $\omega_L = 0.5$. This is equivalent to putting $\omega_{q0} = 0$ and $\omega_L = 0.5$ in our method; however, we prefer to put $\omega_{q0} = -1$ and $\omega_L = 1$ in order to achieve more intrinsic contributions of all terms.

Generally speaking, opposite signs of quantities' changes are not something unusual: for example, a change of velocity at a node may result in changes of the densities at two cells adjacent to this node. Clearly, these changes of densities are of the opposite signs. In view of the state equation, the same is valid for the pressure.

In [4] $\partial\mathrm{Q}_\rho/\partial p^{n+1}$ was obtained numerically due to a small pressure change δp_0, introduced for all cells at the first pass of iteration (see [4], p. 144) and afterwards $\delta\mathrm{Q}_\rho$ was determined. Following our method, this corresponds to $\omega_{p0} = 1$, so in the formula of CRCR an important term vanishes and the iteration procedure will be ineffective for some cases. Obviously, it was cumbersome to set numerically changes of δp_0 that would produce distinct signs at different cells. Therefore a numerical determination of CRCR cannot be *a priori* effective.

We also suppose that the method for obtaining CRCR for an effective Newton iteration procedure can be applied not only to the Navier–Stokes equations.

2. Differential equation

To describe a flow of a viscous heat-conducting gas in the presence of gravity, we use the Navier–Stokes equations in the Eulerian coordinates for the density ρ, the velocity vector $\mathbf{u}(u, v, w)$, and the specific internal energy I along with the state equation for the pressure p:

$$\begin{aligned}
&\frac{\partial\rho}{\partial t} + \mathrm{div}\,\rho\mathbf{u} &&= 0,\\
&\frac{\partial\rho\mathbf{u}}{\partial t} + \mathrm{div}\,\rho\mathbf{u}\mathbf{u} &&= \rho\mathbf{g} - \nabla p + \mathrm{div}\,\mathbf{P}_{\mathrm{visc}}\,,\\
&\frac{\partial\rho I}{\partial t} + \mathrm{div}\,\rho I\mathbf{u} &&= \mathrm{div}\left(\frac{\lambda}{c_V}\nabla I\right) + (\mathbf{P}\cdot\nabla\mathbf{u}),
\end{aligned}$$

$$p = (\gamma_{\text{act}} - 1)\rho(I - I_{\text{noact}}(I)), \tag{1}$$

$$\mathbf{P}_{\text{visc}} \equiv \{\tau_{ij}\} = \left\{-\frac{1}{3}\mu e_{kk}\delta_{ij} + \mu e_{ij}\right\}, \qquad \mathbf{P} = -p\{\delta_{ij}\} + \mathbf{P}_{\text{visc}}, \tag{2}$$

where $\mathbf{g}$ is the gravity acceleration. The components of the strain velocity tensor are as follows:

$$e_{ij} = \partial u_i/\partial x_j + \partial u_j/\partial x_i\,. \tag{3}$$

In Eq. (1) $\gamma_{\text{act}} = c_{P\,\text{act}}/c_{V\,\text{act}}$ means the ratio of thermal capacities for active (translational and rotational) degrees of freedom, while $I_{\text{noact}}(I)$ is determined from the relations:

$$c_{V\,\text{act}} = \frac{1}{\gamma_{\text{act}} - 1}\frac{k}{m}; \qquad I_{\text{act}} = c_{V\,\text{act}}T, \qquad \frac{\mathrm{d}I_{\text{noact}}}{\mathrm{d}T} = c_{V\,\text{noact}}(T),$$
$$I_{\text{noact}}(T = 0) = 0, \qquad I = I_{\text{act}} + I_{\text{noact}}\,. \tag{4}$$

Here k is the Boltzmann constant, m the molecular mass of the gas, and T the absolute temperature.

3. Boundary conditions

To assign the boundary conditions, fictitious boundary cells from the outside of the solution domain are used. A fictitious boundary cell is said to be *degenerate* (possesses zero volume) if it is adjoined to a usual cell from the solid body side. All other fictitious boundary cells are said to be *usual* (have nonzero volume). In Fig. 2 the subscript j, fict, open stands for a fictitious usual cell adjacent to an actual cell j from the side of open boundary. The subscripts j, fict, rig, open and j, fict, rig stand for the fictitious degenerate cells coinciding with the rigid faces of the cells j, fict, open and j, respectively. The subscripts i and i, rig are related to the nodes inside the computation domain and on its wall (on a rigid surface), respectively. The subscripts i, fict and i, fict, rig correspond to respective nodes on the open boundary. All the above cells and nodes may possess the corresponding symmetric cells and nodes, which are not shown in Fig. 2.

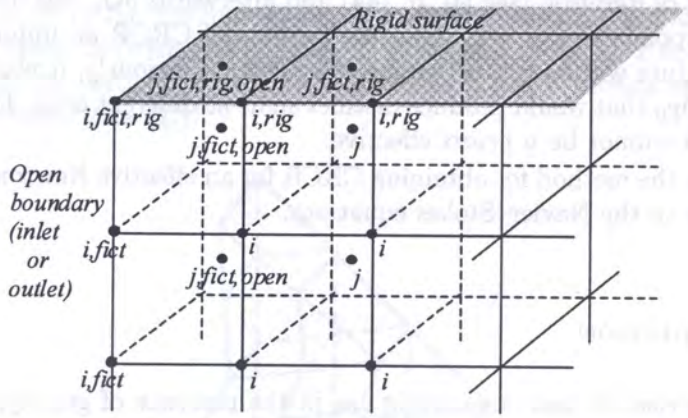

Fig. 2. Schematic representation of positional relationship of the actual and fictitious nodes (i) and cells (j)

On the open boundaries, in the boundary cells j, fict, open the quantities either p, ρ, I or ρ, I must be given. In case of p, ρ, I given, the velocity $\mathbf{u}$ at the boundary nodes i, fict and i, fict, rig will be defined by assigning their values at the internal nodes i and i, rig, where the velocities are known via calculation. This is necessary in order to calculate the strain velocity tensors in the boundary cells j, fict, open. These tensors are then applied to calculate the viscous stress tensors at the nodes i. The open boundaries are assumed to be sufficiently distant from domains possessing

high gradients. In the case where only ρ, I are given in the cells j, fict, open, the velocities must be *a priori* given at the nodes i, fict and i, fict, rig, and at the adjacent nodes i and i, rig.

To calculate the parameters of a gas moving in open devices, we used the continuity condition of the flow near the open boundary (see [5]) and the presence of gravity. Therefore the boundary conditions

$$p_{j,\,\mathrm{fict,\,open}} = (1-\Delta t/\tau)p_j e^{\mathbf{g}\cdot(\mathbf{r}_{j,\,\mathrm{fict,\,open}}-\mathbf{r}_j)\rho_j/p_j} + (\Delta t/\tau)p_\infty e^{\mathbf{g}\cdot(\mathbf{r}_{j,\mathrm{fict,\,open}}-\mathbf{r}_\infty)\rho_\infty/p_\infty},$$

$$I_{j,\,\mathrm{fict,\,open}} = (1-\Delta t/\tau)I_j + (\Delta t/\tau)I_\infty$$

were taken into account. The value $\rho_{j,\,\mathrm{fict,\,open}}$ is determined via $p_{j,\,\mathrm{fict,\,open}}$ and $I_{j,\,\mathrm{fict,\,open}}$ through the state equation. The values ρ_∞ and p_∞ are the density and pressure, respectively, at infinity at a given height which is defined by a position vector $\mathbf{r}_\infty$. For a viscous steady flow in a tube, the spatial pressure distribution for $\Delta t/\tau < 1$ is same as for $\Delta t/\tau = 1$ if the tube length has been extended by $(\tau/\Delta t)h$ in the output direction. The relaxation parameter $\Delta t/\tau$ is taken equal to 0.01.

In contrast to [2], $\nabla I_{i,\,\mathrm{rig}}$ at the nodes i, rig lying on a solid surface are calculated by means of the Newton-type iteration scheme so that ∇I_j (defined from $\nabla I_{i,\,\mathrm{rig}}$) in the cells j near the solid surface is equal to ∇I_j calculated via the given values $I_{i,\,\mathrm{rig}}$. At rigid walls, for $\mu \neq 0$, we put $\mathbf{u} = 0$.

4. Grid, nodes, faces and cells, finite difference approximation of differential operators and other terms

In this section we give formulas for finite difference approximations, which are obtained for cell faces given in specific ways. However, these formulas possess a well-known universal form admissible for various shapes of the cell faces. The distinct shapes generate different geometric coefficients $\mathbf{c}$. The formulas of CRCR can use different geometric coefficients corresponding to different choice of cells. Note that different geometric coefficients can be used in the calculation of both CRCR and the residuals. Let us note that an approximate equivalence between cells used for calculation and constructed in different ways around the same point is important. However, in calculation of the residuals the kind of both difference schemes for approximation of spatial operators and applied geometric coefficients is also important, because may change the time step and computation time of the Newton iteration procedure.

4.1. Nodes, faces and cells

The faces and geometric coefficient $\mathbf{c}^l$ at a point l are constructed in the following way. We define the face m as a surface passing through given edges. The geometric coefficient $\mathbf{c}^m$ is set to be equal to the surface normal vector directed outside from the cell:

$$\mathbf{c}^m = \int_{S_m} \mathrm{d}\boldsymbol{\sigma}.$$

Draw a plane perpendicular to $\mathbf{c}^m$. Next, drop perpendiculars onto this plane from the vertices l of the face m. Next, for the resulting plane polygon we find the centroid (centre of gravity) O.

The polygon is divided into a set of quadrangles (see in Fig. 3). The ratio of the square of the quadrangle $L_1 L L_2 O$ (L_1 and L_2 are the middles of polygon's edges) to the square of the polygon gives us the quantity q^{ml}

$$q^{ml} = \frac{S_{L_1 L L_2 O}}{c^m}, \qquad \sum_l q^{ml} = 1. \tag{5}$$

The face m can be considered as a set of triangles mnl with a point m defined as

$$\mathbf{r}_m = \sum_{l=1}^{N_m} q^{ml}\mathbf{r}_l\,. \tag{6}$$

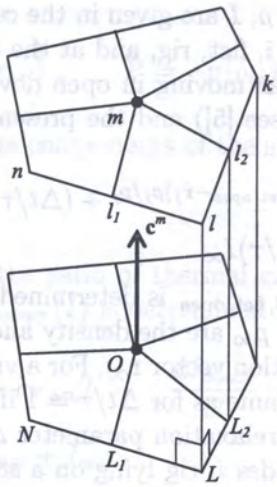

Fig. 3. The projection of the face m is a plane polygon

Here N_m is the number of vertices of the face m. In other words, S_m is a surface obtained by rotation of a straight-line segment around the point m, so that the end of segment runs over the straight edges. For the sake of simplicity, here and in some places in what follows, the limits of sums will be omitted.

Let us establish some properties of the face S_m. Consider a S_M as a set of triangles Mnl with an arbitrary point M which may coincide with m or O (or any other point); we then have for the dyad tensor:

$$\int_{S_M} \mathbf{r}\,\mathrm{d}\boldsymbol{\sigma} = \frac{1}{3}\sum_l (\mathbf{r}_M + \mathbf{r}_n + \mathbf{r}_l)\boldsymbol{\sigma}_{nlM} = \frac{\mathbf{r}_M}{3}\sum_n \boldsymbol{\sigma}_{nlM} + \frac{1}{3}\sum_n \mathbf{r}_n 2\boldsymbol{\sigma}_{nl_1M} + \frac{1}{3}\sum_l \mathbf{r}_l 2\boldsymbol{\sigma}_{l_1lM}$$

$$= \frac{\mathbf{r}_M \mathbf{c}^m}{3} + \frac{2}{3}\sum_l \mathbf{r}_l \boldsymbol{\sigma}_{ll_2M} + \frac{2}{3}\sum_l \mathbf{r}_l 2\boldsymbol{\sigma}_{l_1lM}\,.$$

Hence it follows

$$\int_{S_M} \mathbf{r}\,\mathrm{d}\boldsymbol{\sigma} = \frac{\mathbf{r}_M \mathbf{c}^m}{3} + \frac{2}{3}\sum_l \mathbf{r}_l \boldsymbol{\sigma}_{l_1ll_2M}\,. \tag{7}$$

Here l_1 and l_2 are the middles of the edges nl and lk, respectively, $\boldsymbol{\sigma}_{l_1ll_2M}$, $\boldsymbol{\sigma}_{l_1lM}$, and $\boldsymbol{\sigma}_{ll_2M}$ are the surface normal vectors of the quadrangle l_1ll_2M and the triangles l_1lM, and ll_2M, respectively.

Let us prove that

$$\mathbf{r}_{mO} = \mathbf{r}_m - \mathbf{r}_O \parallel \mathbf{c}^m. \tag{8}$$

Using (7) for plane polygon with the points O, L ($L = 1, N_m$) taken instead of M, l ($l = 1, N_m$), respectively, we obtain

$$\mathbf{r}_O \mathbf{c}^m = \frac{\mathbf{r}_O \mathbf{c}^m}{3} + \frac{2}{3}\sum_l \mathbf{r}_L \boldsymbol{\sigma}_{L_1LL_2O} \;\Rightarrow\; \mathbf{r}_O \mathbf{c}^m = \sum_l \mathbf{r}_L S_{L_1LL_2O}\frac{\mathbf{c}^m}{c^m},$$

which in view of Eqs. (5) and (6) gives us

$$\mathbf{r}_O = \sum_l q^{ml}\mathbf{r}_L \qquad \text{and} \qquad \mathbf{r}_{mO} = \sum_l q^{ml}\mathbf{r}_{lL}\,.$$

Since $\mathbf{r}_{lL} = \mathbf{r}_l - \mathbf{r}_L \parallel \mathbf{c}^m$, (8) has been proved.

Prove that the point $\mathbf{r}_m$ of the face m is determined only by boundary straight edges and the result of (6) does not depend on the number N_m of the point l. In other words, the insertion of additional vertices into the boundary straight edges does not change $\mathbf{r}_m$ and therefore the face m. For any point M on a perpendicular to the quadrangle L_1LL_2O, in point O from Eqs. (5) and (6) we have

$$q^{ml} = \frac{\boldsymbol{\sigma}_{l_1 l l_2 M} \cdot \mathbf{c}^m}{(c^m)^2}; \qquad \mathbf{r}_m = \sum_l \mathbf{r}_l \frac{\boldsymbol{\sigma}_{l_1 l l_2 M} \cdot \mathbf{c}^m}{(c^m)^2}. \tag{9}$$

Since

$$2\boldsymbol{\sigma}_{l_1 l l_2 M} = \boldsymbol{\sigma}_{nlM} + \boldsymbol{\sigma}_{lkM},$$

we obtain that

$$2\sum_l \mathbf{r}_l \boldsymbol{\sigma}_{l_1 l l_2 M} = \sum_l \mathbf{r}_l \boldsymbol{\sigma}_{nlM} + \sum_l \mathbf{r}_n \boldsymbol{\sigma}_{nlM} = \sum_l (\mathbf{r}_n + \mathbf{r}_l) \frac{\mathbf{r}_{nM} \times \mathbf{r}_{lM}}{2}.$$

This instead of (9) gives us

$$\mathbf{r}_m = \sum_l \frac{\mathbf{r}_n + \mathbf{r}_l}{2} \frac{\mathbf{r}_{nM} \times \mathbf{r}_{lM}}{2} \cdot \frac{\mathbf{c}^m}{(c^m)^2}. \tag{10}$$

Clearly, the following expression

$$\mathbf{r}_m = \oint \mathbf{r} \frac{(\mathbf{r} - \mathbf{r}_M) \times \mathrm{d}\mathbf{r}}{2} \cdot \frac{\mathbf{c}^m}{(c^m)^2} \tag{11}$$

is independent of both the choice of vertices on given boundary straight edges and the choice of a point M on a given perpendicular to the quadrangle LL_1L_2O at the point O, because $\mathbf{r}_{MO} = \mathbf{r}_M - \mathbf{r}_O \parallel \mathbf{c}^m$. Let us show that (11) produces the same result as (10) does. In Eq. (11) the contour integral is taken along a closed contour consisting of straight edges connecting the points $\mathbf{r}_n$ and $\mathbf{r}_l$ ($l = 1, 2, \ldots N_m$). Since $\mathbf{r} - \mathbf{r}_l \parallel \mathrm{d}\mathbf{r}$ for $\mathbf{r} \in [\mathbf{r}_n, \mathbf{r}_l]$, instead of (11) we have

$$\mathbf{r}_m = \sum_l \int_{\mathbf{r}_n}^{\mathbf{r}_l} \mathbf{r} \frac{(\mathbf{r}_l - \mathbf{r}_M) \times \mathrm{d}\mathbf{r}}{2} \cdot \frac{\mathbf{c}^m}{(c^m)^2} = -\sum_l \left[\int_{\mathbf{r}_n}^{\mathbf{r}_l} \mathbf{r}\,\mathrm{d}\mathbf{r} \times \frac{\mathbf{r}_{lM}}{2} \right] \cdot \frac{\mathbf{c}^m}{(c^m)^2}. \tag{12}$$

Let us evaluate the (i, j)-th component of the dyad tensor

$$\int_{\mathbf{r}_n}^{\mathbf{r}_l} x_i \,\mathrm{d}x_j = \frac{x_{lj} - x_{nj}}{x_{li} - x_{ni}} \int_{\mathbf{r}_n}^{\mathbf{r}_l} x_i \,\mathrm{d}x_i = \frac{x_{lj} - x_{nj}}{x_{li} - x_{ni}} \frac{(x_{li})^2 - (x_{ni})^2}{2} = \frac{x_{ni} + x_{li}}{2} (x_{lMj} - x_{nMj}).$$

Here $x_{lMj} = x_{lj} - x_{Mj}$ is the j-th component of the vector $\mathbf{r}_{lM} = \mathbf{r}_l - \mathbf{r}_M$. Now Eq. (12) turns into the new relation

$$\mathbf{r}_m = -\sum_l \frac{(\mathbf{r}_n + \mathbf{r}_l)}{2} \frac{(\mathbf{r}_{lM} - \mathbf{r}_{nM}) \times \mathbf{r}_{lM}}{2} \cdot \frac{\mathbf{c}^m}{(c^m)^2},$$

which after simplification will coincide with (10). Thus we have obtained the desired result.

The following property of the face S_m is also of interest. Let $S_{m\perp}$ be the projection of S_m onto the plane that passes through m and is perpendicular to $\mathbf{c}^m$. The volumes between S_m and $S_{m\perp}$ on the opposite sides of $S_{m\perp}$ are equal to each other.

4.2. Finite difference approximation

Here we derive the formulas for finite difference approximation of differential operators and for determination of quantities in a cell provided that the quantities are known at the cell vertices. We also give an estimate of approximation inaccuracy for various faces, cells, and geometric coefficients.

Since (8), Eq. (9) with m instead of Mgives us

$$\left(\mathbf{c}^m q^{ml} - \boldsymbol{\sigma}_{l_1 l l_2 m}\right) \cdot \mathbf{c}^m = 0.$$

If we substitute Eq. (6) into (7) with m taken instead of M, then we have

$$\int_{S_m} \mathbf{r}\, \mathrm{d}\boldsymbol{\sigma} = \sum_l \mathbf{r}_l \mathbf{c}^{ml}, \tag{13}$$

where the geometric coefficient $\mathbf{c}^{ml}$ of the face m at the point l is as follows

$$\mathbf{c}^{ml} = \frac{\mathbf{c}^m q^{ml} + 2\boldsymbol{\sigma}_{l_1 l l_2 m}}{3}. \tag{14}$$

Clearly, from (13) we have

$$\int_{S_m} \mathbf{r} \cdot \mathrm{d}\boldsymbol{\sigma} = \sum_l \mathbf{r}_l \cdot \mathbf{c}^{ml}. \tag{15}$$

In view of (6) and

$$\mathbf{c}^m = \sum_l \boldsymbol{\sigma}_{l_1 l l_2 m} \qquad \text{and} \qquad \mathbf{r}_l \cdot \boldsymbol{\sigma}_{l_1 l l_2 m} = \mathbf{r}_m \cdot \boldsymbol{\sigma}_{l_1 l l_2 m},$$

for the general case of non-planar face, from formulas (15) and (14) we have

$$\int_{S_m} \mathbf{r} \cdot \mathrm{d}\boldsymbol{\sigma} = \sum_l \mathbf{r}_l \cdot \mathbf{c}^{ml} = \mathbf{r}_m \cdot \mathbf{c}^m = \sum_l \mathbf{r}_l \cdot q^{ml} \mathbf{c}^m = \sum_l \mathbf{r}_l \cdot \boldsymbol{\sigma}_{l_1 l l_2 m}.$$

Clearly,

$$\int_{S_m} \mathrm{d}\boldsymbol{\sigma} = \mathbf{c}^m = \sum_l \mathbf{c}^{ml} = \sum_l q^{ml} \mathbf{c}^m = \sum_l \boldsymbol{\sigma}_{l_1 l l_2 m}. \tag{16}$$

Next, for the surface S of a cell with the number of faces N_f, we have

$$\int_S \mathrm{d}\boldsymbol{\sigma} = \sum_{m=1}^{N_f} \mathbf{c}^m = \sum_{m=1}^{N_f} \sum_{l=1}^{N_m} \mathbf{c}^{ml} = \sum_{m=1}^{N_f} \sum_{l=1}^{N_m} q^{ml} \mathbf{c}^m = \sum_{m=1}^{N_f} \sum_{l=1}^{N_m} \boldsymbol{\sigma}_{l_1 l l_2 m} = 0. \tag{17}$$

In the case of a planar cell face, we have

$$\mathbf{c}^{ml} = \mathbf{c}^m q^{ml} = \boldsymbol{\sigma}_{l_1 l l_2 m}.$$

For the general case of non-planar face, these vectors differ by both their magnitude and direction. The relative difference may be characterized by the quantity Δ_{face}, which characterizes also the nonflatness of the face

$$\Delta_{\text{face}} = \max_l \frac{|\mathbf{r}_{lm} \cdot \mathbf{c}^m|}{r_{lm} c^m}.$$

Let us denote by $\mathbf{c}^l$ the geometric coefficient at vertex l of the cell; $\mathbf{c}^l$ consists of components $\mathbf{c}^{ml}$ related to every face m which passes through the vertex l

$$\mathbf{c}^l = \sum_m \mathbf{c}^{ml}. \tag{18}$$

For hexahedrons with planar faces, it can be shown that the expression for $\mathbf{c}^l$ coincides with the formula suggested by D. C. Barnes in [6]. Coefficient $\mathbf{c}^l$ has a clear geometric meaning. In case of a cell with planar faces, it is the sum of the three vectors normal to the respective faces and possessing lengths equal to the areas of quadrangles. Any quadrangle is a part of the respective face and has the four vertices: the vertex l of the cell, the two centres (middles) of edges, and the face's centroid. Three of these quadrangles for the coefficient $\mathbf{c}^4$ are shown by hatching in Fig. 4.

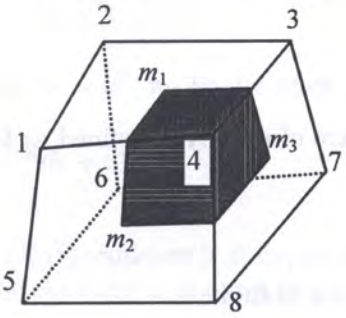

Fig. 4. A geometric interpretation of the coefficient $\mathbf{c}^4$

By using the above-mentioned geometric coefficients, we may obtain the finite difference form of quantities. We approximate the gradient of Φ at the cell by the average value over the cell and, by means of the Gauss theorem, transform the volume integral into a surface integral (see [1]):

$$\nabla\Phi = \frac{1}{V}\int_V \nabla\Phi \,\mathrm{d}V = \frac{1}{V}\int_V [\mathbf{i}\,\mathrm{div}(\Phi\mathbf{i}) + \mathbf{j}\,\mathrm{div}(\Phi\mathbf{j}) + \mathbf{k}\,\mathrm{div}(\Phi\mathbf{k})]\,\mathrm{d}V = \frac{1}{V}\int_S \Phi\,\mathrm{d}\boldsymbol{\sigma}. \tag{19}$$

In this case, we can approximate a surface integral by the sum of the products of Φ and the geometric coefficients $\mathbf{c}^l$:

$$\nabla\Phi = \frac{1}{V}\sum_{l=1}^{N} \Phi_l \mathbf{c}^l. \tag{20}$$

Here N stands for the number of cell vertices.

In what follows we will show that the surface integral in Eq. (19) gives us the gradient of Φ at the centre of gravity M with an inaccuracy of the second order with respect to h. We will also show that formula (20) represents the gradient of Φ at the centre of gravity M with an inaccuracy of the second order with respect to h for a cell generated by pairs of faces coinciding with each other after a parallel translation. For other cells the inaccuracy will be of the first order with respect to h.

First of all let us obtain formulas for the cell volume and the position vector $\mathbf{r}_M$ of the centre of gravity M. Using the Gauss theorem and (13), (18), we obtain

$$V = \int_V \mathrm{d}V = \int_V \mathrm{div}\,(x\mathbf{i})\,\mathrm{d}V = \int_S (x\mathbf{i})\cdot\mathrm{d}\boldsymbol{\sigma} = \int_S x\,\mathrm{d}\sigma_x = \sum_l x_l c_x^l. \tag{21}$$

Similarly,

$$V = \sum_{l=1}^{N} x_l c_x^l = \sum_{l=1}^{N} y_l c_y^l = \sum_{l=1}^{N} z_l c_z^l = \frac{1}{3}\sum_{l=1}^{N} \mathbf{r}_l \cdot \mathbf{c}^l. \tag{22}$$

Since, for example, $\operatorname{div}(x\mathbf{j}) = \operatorname{div}(\mathbf{j}) = 0$, we have as in (21) and with regard for (17):

$$\sum_{l=1}^{N} y_l c_x^l = \sum_{l=1}^{N} z_l c_x^l = ... = \sum_{l=1}^{N} y_l c_z^l = \sum_{l=1}^{N} c_x^l = \sum_{l=1}^{N} c_y^l = \sum_{l=1}^{N} c_z^l = \sum_{l=1}^{N} \mathbf{c}^l = 0. \tag{23}$$

We also will need the following formula implied from (13) and (18)

$$\int_S \mathbf{r}\,\mathrm{d}\boldsymbol{\sigma} = \sum_{l=1}^{N} \mathbf{r}_l \mathbf{c}^l,$$

which along with (22) and (23) gives us

$$\frac{1}{V}\sum_{l=1}^{N} \mathbf{r}_l \mathbf{c}^l = \frac{1}{V}\sum_{l=1}^{N} \mathbf{c}^l \mathbf{r}_l = \mathbf{E},$$

where $\mathbf{E}$ is the unit tensor. The centre of gravity is defined as follows

$$\mathbf{r}_M = \frac{1}{V}\int_V \mathbf{r}\,\mathrm{d}V. \tag{24}$$

Applying again the Gauss theorem, we obtain

$$\mathbf{r}_M = \frac{1}{4V}\int_V \operatorname{div}(\mathbf{rr})\,\mathrm{d}V = \frac{1}{4V}\int_S \mathbf{rr}\cdot\mathrm{d}\boldsymbol{\sigma} = \frac{1}{4V}\sum_m \int_{S_m} \mathbf{rr}_m \cdot \mathrm{d}\boldsymbol{\sigma} = \frac{1}{4V}\sum_m \mathbf{r}_m \cdot \int_{S_m} \mathrm{d}\boldsymbol{\sigma}(\mathbf{r}).$$

Therefore from (13) we have

$$\mathbf{r}_M = \frac{1}{4V}\sum_m \mathbf{r}_m \cdot \sum_l \mathbf{c}^{ml}\mathbf{r}_l\,.$$

Now let us obtain the formula for the quantity Φ_M at the centre of gravity. Note that, if

$$\mathbf{r}_A = \sum_l A_l \mathbf{r}_l \qquad \text{and} \qquad \sum_l A_l = 1,$$

then

$$\Phi_A = \sum_l A_l \Phi_l + O(h^2),$$

as one can easily check by the multivariable Taylor expansion in Φ_A

$$\Phi = \Phi_A + \nabla\Phi_A \cdot (\mathbf{r} - \mathbf{r}_A) + O(h^2). \tag{25}$$

The remainder term $O(h^2)$ is equal to zero if the dependence of Φ on the space coordinates is linear.

Therefore in view of (24) the following equation takes place:

$$\Phi_M = \frac{1}{V}\int_V \Phi\,\mathrm{d}V + O(h^2). \tag{26}$$

Since

$$\Phi = \frac{1}{3}\operatorname{div}[\Phi(\mathbf{r} - \mathbf{r}_M)] - \frac{1}{3}\nabla\Phi\cdot(\mathbf{r} - \mathbf{r}_M)$$

and

$$\mathbf{r}-\mathbf{r}_M = O(h), \quad \nabla\Phi = \nabla\Phi_M + O(h) \quad \text{for } \mathbf{r}\in \text{cell } V, \qquad \mathbf{r}-\mathbf{r}_m \perp \mathrm{d}\boldsymbol{\sigma} \quad \text{for } \mathbf{r}\in \text{face } m,$$

from (26) by applying the Gauss theorem and (24) we have:

$$\Phi_M = \frac{1}{3V}\int_S \Phi(\mathbf{r}-\mathbf{r}_M)\cdot \mathrm{d}\boldsymbol{\sigma} + O(h^2) = \frac{1}{3V}\sum_m (\mathbf{r}_m-\mathbf{r}_M)\cdot\int_{S_m}\Phi\,\mathrm{d}\boldsymbol{\sigma} + O(h^2).$$

By using the multivariable Taylor expansion with Φ_m taken instead of Φ_A in (25), by substituting (16) and (13) into the last integral, we obtain

$$\int_{S_m}\Phi\,\mathrm{d}\boldsymbol{\sigma} = \sum_l \Phi_m \mathbf{c}^{ml} + \nabla\Phi_m\cdot\sum_l(\mathbf{r}_l-\mathbf{r}_m)\mathbf{c}^{ml} + \mathbf{O}(h^2)c^m = \sum_l \Phi_l\mathbf{c}^{ml} + \mathbf{O}(h^2)c^m,$$

and, taking into account $c^m \sim h^2$ and $V\sim h^3$, we finally have

$$\Phi_M = \frac{1}{3V}\sum_m(\mathbf{r}_m-\mathbf{r}_M)\cdot\sum_l \mathbf{c}^{ml}\Phi_l + O(h^2).$$

We recall that the remainder term $O(h^2)$ vanishes if Φ depends linearly on the space coordinates. The same formulas for V or $\mathbf{r}_M$ can be obtained in another way if instead of Φ in the above expression one takes 1 or $\mathbf{r}$, respectively.

If we apply Eq. (26) to $\nabla\Phi_M$ instead of Φ_M, then we have

$$\nabla\Phi_M = \frac{1}{V}\int_V \nabla\Phi\,\mathrm{d}V + \mathbf{O}(h^2) = \frac{1}{V}\int_S \Phi\,\mathrm{d}\boldsymbol{\sigma} + \mathbf{O}(h^2), \tag{27}$$

where the reminder term $O(h^2)$ vanishes if the $\nabla\Phi$ depends linearly on the space coordinates and, consequently, the Φ has a quadratic dependence on the space coordinates.

To determine the inaccuracy of formula (20), we consider the surface S consisting of S_m and replace Φ in (27) with its Taylor expansion in Φ_m

$$\Phi = \Phi_m + \nabla\Phi_m\cdot(\mathbf{r}-\mathbf{r}_m) + \frac{1}{2}\sum_{i=1}^3\sum_{j=1}^3 \frac{\partial^2\Phi_m}{\partial x_i\partial x_j}(x_i-x_{mi})(x_j-x_{mj}) + O(h^3).$$

Applying also (16) and (13), we obtain

$$\begin{aligned}\nabla\Phi_M = {} & \frac{1}{V}\sum_m\sum_l \Phi_m\mathbf{c}^{ml} + \frac{1}{V}\sum_m\sum_l \nabla\Phi_m\cdot(\mathbf{r}_l-\mathbf{r}_m)\mathbf{c}^{ml} \\ & + \frac{1}{2}\sum_{i=1}^3\sum_{j=1}^3\sum_m \frac{\partial^2\Phi_m}{\partial x_i\partial x_j}\frac{1}{V}\int_{S_m}(x_i-x_{mi})(x_j-x_{mj})\,\mathrm{d}\boldsymbol{\sigma} + \frac{1}{V}\int_S O(h^3)\,\mathrm{d}\boldsymbol{\sigma} + \mathbf{O}(h^2).\end{aligned}$$

The order of the remainder term will not do be deteriorated if we replace the partial derivative of the second order at the point m with the derivative at the point M. Straightforward simplification gives us

$$\begin{aligned}\nabla\Phi_M = {} & \frac{1}{V}\sum_m\sum_l \Phi_l\mathbf{c}^{ml} + \mathbf{O}(h^2) \\ & + \frac{1}{2}\sum_{i=1}^3\sum_{j=1}^3 \frac{\partial^2\Phi_M}{\partial x_i\partial x_j}\frac{1}{V}\sum_m\left[\int_{S_m}(x_i-x_{mi})(x_j-x_{mj})\,\mathrm{d}\boldsymbol{\sigma} - \sum_l (x_{li}-x_{mi})(x_{lj}-x_{mj})\mathbf{c}^{ml}\right].\end{aligned} \tag{28}$$

The last term in (28) vanishes for a cell generated by pairs of parallel faces. This is obvious because for the corresponding opposite faces the vectors $\mathrm{d}\boldsymbol{\sigma}$ or $\mathbf{c}^{ml}$ are equal by their absolute value but are oppositely directed, while remaining multipliers coincide. To the cells with pairwise parallel faces we assign the parameter $\Delta_{\text{cell}} = 0$, while $\Delta_{\text{cell}} = 1$ for all other cells. Thus, by substituting (18) into (28), we can rewrite (28) as follows

$$\nabla \Phi_M = \frac{1}{V} \sum_l \Phi_l \mathbf{c}^l + \Delta_{\text{cell}} \mathbf{O}(h) + \mathbf{O}(h^2). \tag{29}$$

From (29) it directly follows that

$$\operatorname{div} \boldsymbol{\Phi}_M = \frac{1}{V} \sum_l \boldsymbol{\Phi}_l \cdot \mathbf{c}^l + \Delta_{\text{cell}} O(h) + O(h^2).$$

Thus we can see that the central difference scheme (CDS) can supply a first order truncation error in h if $\Delta_{\text{cell}} = 1$. The truncation error of the second order in h is equal to zero if Φ depends on the space coordinates in quadratic form; however, an error of the first order in h remains if $\Delta_{\text{cell}} = 1$. If the dependence of Φ on the space coordinates is linear, then the error vanishes for any Δ_{cell}.

In determination of the divergence, the inaccuracy of the upwind difference scheme (UDS) will be of the first order in h and of the first order in Δ_{mesh}, Δ_{mesh} characterizes the nonuniformity of the mesh spacing, i.e., the difference between the adjacent cells j and j'

$$\Delta_{\text{mesh}} \approx \frac{h_{j'}}{h_j} - 1.$$

If we introduce $\Delta_{\text{UDS}} = 1$ in case of UDS scheme is used and $\Delta_{\text{UDS}} = 0$ in case of CDS scheme, then

$$\operatorname{div} \boldsymbol{\Phi}_M = \frac{1}{V} \sum_l \boldsymbol{\Phi}_l \cdot \mathbf{c}^l + (\Delta_{\text{mesh}} + O(h)) \Delta_{\text{UDS}} + \Delta_{\text{cell}} O(h) + O(h^2). \tag{30}$$

For a more accurate calculation, the quantities V and $\mathbf{r}_M$ will be determined from the formulas

$$V = \sum_{l=1}^{N} (x_l - x_1) c_x^l = \sum_{l=1}^{N} (y_l - y_1) c_y^l = \sum_{l=1}^{N} (z_l - z_1) c_z^l \quad \text{or} \quad V = \frac{1}{3} \sum_{l=1}^{N} (\mathbf{r}_l - \mathbf{r}_1) \cdot \mathbf{c}^l$$

and

$$\mathbf{r}_M = \mathbf{r}_1 + \frac{1}{4V} \sum_m (\mathbf{r}_m - \mathbf{r}_1) \cdot \sum_l \mathbf{c}^{ml} (\mathbf{r}_l - \mathbf{r}_1). \tag{31}$$

If we will use $q^{ml} \mathbf{c}^m$ instead of $\mathbf{c}^{ml}$, the corresponding geometric coefficient $\mathbf{c}_0^l$

$$\mathbf{c}_0^l = \sum_m q^{ml} \mathbf{c}^m$$

will appear instead of $\mathbf{c}^l$. After a simplification, the formulas can be expressed as follows:

$$V = \frac{1}{3} \sum_{l=1}^{N} (\mathbf{r}_l - \mathbf{r}_1) \cdot \mathbf{c}_0^l, \tag{32}$$

$$\mathbf{r}_M = \mathbf{r}_1 + \frac{1}{4V} \sum_{l=1}^{N} (\mathbf{r}_l - \mathbf{r}_1) \left((\mathbf{r}_l - \mathbf{r}_1) \cdot \mathbf{c}_0^l \right) + \Delta_{\text{face}} \mathbf{O}(h), \quad |\mathbf{O}(h)| \approx h, \tag{33}$$

$$\Phi_M = \frac{1}{3V}\sum_{l=1}^{N}\left((\mathbf{r}_l - \mathbf{r}_M)\cdot\mathbf{c}_0^l\right)\Phi_l + \Delta_{\text{face}}\nabla\Phi_M\cdot\mathbf{O}(h) + O(h^2), \quad |\mathbf{O}(h)| \approx h, \tag{34}$$

$$\nabla\Phi_M = \frac{1+\Delta_{\text{face}}O(1)}{V}\sum_l \Phi_l\mathbf{c}_0^l + \Delta_{\text{cell}}\mathbf{O}(h) + \mathbf{O}(h^2), \quad O(1)\approx 1,$$

$$|\mathbf{O}(h)| \approx h\sum_{i=1}^{3}\sum_{j=1}^{3}\left|\frac{\partial^2\Phi}{\partial x_i x_j}\right|, \tag{35}$$

$$\text{div}\boldsymbol{\Phi}_M = \frac{1+\Delta_{\text{face}}O(1)}{V}\sum_l \boldsymbol{\Phi}_l\cdot\mathbf{c}_0^l + \Delta_{\text{cell}}O(h) + O(h^2), \quad |O(h)| \approx h\sum_{i=1}^{3}\sum_{j=1}^{3}\left|\frac{\partial^2\boldsymbol{\Phi}}{\partial x_i x_j}\right|. \tag{36}$$

In Eq. (34) the vector $\mathbf{r}_M$ is taken from (33) as determined approximately. One can see that additional inaccuracies appear in the formulas (with except for Eq. (32)). These formulas do not compute and remember $\mathbf{r}_m$ and vectors $\mathbf{c}^{ml}$; they deal only with the scalars q^{ml} and vectors $\mathbf{c}^m$, so they save the memory. They can be used for the computation of the residuals if $\Delta_{\text{face}} \ll 1$; however, the geometric coefficients $\mathbf{c}_0^l$ can always be used to compute CRCR.

4.3. Displaced cells, finite difference approximation

The above formulas make it possible to write the Navier–Stokes equations in a finite difference form. Some terms in the finite-difference equations can be obtained with the use of the above cell. Other terms, especially those corresponding to the finite-difference equation for $\mathbf{u}$, use displaced cells which are constructed around the nodes. The displaced cell around the node is composed of pieces of the usual cells surrounding the node. The displaced cell used in [4, 6] is shown in Fig. 5 by the dotted line. Here the displaced cell vertices are the centroids of the usual cells surrounding the node i. In the Fig. 5, the numbers are assigned not to the vertices of a usual cell but to the displaced cell vertices. In this figure, like in Fig. 4, we hatched the same part of the usual cell surface. The unhatched part of surface of cell $6m_1m_2m_3$ ($Mm_1m_2m_3$ in Fig. 4) gives us a part of the displaced cell surface. This part consists of quadrangles. Every quadrangle has the four vertices: a centroid of the usual cell, the centre (middle) of the edge, and the two centroids of adjacent faces having this common edge. We denote by $\mathbf{c}'$ the coefficient $\mathbf{c}$ for the displaced cell. In [4], the coefficient $\mathbf{c}'$ for the displaced cell around the node and the corresponding coefficient $\mathbf{c}$ for a usual cell from the set of cells surrounding the node are assumed to be equal in their magnitudes and oppositely directed.

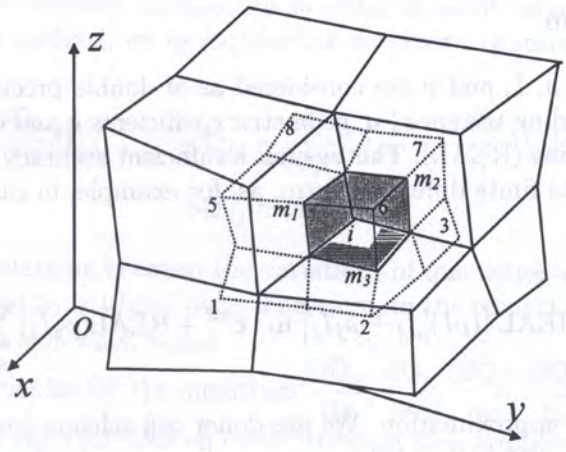

Fig. 5. A displaced cell around the node i

This will take place if the geometric coefficient $\mathbf{c}$ for the usual cell and coefficient $\mathbf{c}'$ for the displaced cell will be taken as the sums of the vectors normal to their respective faces and possessing lengths equal to the areas of the respective quadrangles. Such quadrangles for the corresponding coefficients $\mathbf{c}$ and $\mathbf{c}'$ form a cell; so $\mathbf{c}' = -\mathbf{c}$.

The use of such displaced cells and geometric coefficients $\mathbf{c}'$ in a finite difference approximation gives rise to a significant computational error. Therefore these cells and values will be called "bad cells" and "bad geometric coefficients $\mathbf{c}'$", respectively. As was mentioned in [6], if the pressure is constant in the whole space, then by (29) and (23) for a displaced cell we have $\nabla p = 0$, i.e. the node has no acceleration. It is of interest to see what will happen if the bad displaced cells will be used in the case $\nabla p = \text{const}$. It turns out that uncompensated forces appear in the momentum equation if the displaced cells have composite faces in accordance with the requirement $\mathbf{c}' = -\mathbf{c}$. In particular, the verification for a gas in equilibrium in a gravitational field demonstrated that the uncompensated force acting on a bad displaced cell is equal to $\alpha\rho g V$, where V is the cell volume, and α is a coefficient characterizing an irregularity rate of the faces of the displaced cell. Next, α gives us the same error in the computation as Δ_{face} if the coefficient $\mathbf{c}_0^l$ is used instead of $\mathbf{c}^l$ (see Eqs. (33)–(36)). Note that α may be as high as $0.1 \div 0.2$.

Thus, instead of the bad displaced cells we will use other displaced cells, called "good" ones. As the usual cells, these are also determined only by vertices. These vertices are the centroids of the usual cells surrounding the node. For such displaced cells, their coefficients $\mathbf{c}'$ are defined in Eqs. (14), (18); however, for the new cells the position vectors $\mathbf{r}_l$ will be used as centroids. By means of the bad both displaced cells and geometric coefficients $\mathbf{c}'$, we find the approximate correlation $\mathbf{c}' \approx -\mathbf{c}$ between the corresponding good geometric coefficient $\mathbf{c}'$ of good displaced cell and the coefficient $\mathbf{c}$ of the usual cell. This correlation will be used in the determination of CRCR.

For correct computation we need to know the difference between a node i and the centroid (centre of gravity) M of a displaced cell around the node i. The relative difference can be characterized by the following quantity:

$$\Delta_{\text{displace}} = \frac{|\mathbf{r}_i - \mathbf{r}_M|}{h}.$$

This quantity is close to Δ_{mesh}. If we do not use Eq. (31) for displaced cell and instead of $\mathbf{r}_M$ the position vector $\mathbf{r}_i$ of node i will be taken, then an additional inaccuracy term $\Delta_{\text{displace}} O(h)$ appears in the corresponding formulas. For example, Eq. (29) gives us

$$\nabla\Phi_i = \frac{1}{V}\sum_l \Phi_l \mathbf{c}^l + (\Delta_{\text{cell}} + \Delta_{\text{displace}})\mathbf{O}(h) + \mathbf{O}(h^2).$$

4.4. Accuracy estimation

In the program the values ρ, I, and p are considered as of double precision, meanwhile almost all remaining quantities (including the speed $\mathbf{u}$, geometric coefficients $\mathbf{c}$ and $\mathbf{c}'$, and the coordinates) are taken with the single precision (REAL). This ensures a sufficient accuracy if we assign the differential operators in the appropriate finite difference form, as, for example, in case of the convective flux of energy

$$\operatorname{div} \rho I \mathbf{u}_j = \frac{1}{V_j}\left\{\sum_{m,l} \text{REAL}\left[(\rho I)'_{m,l} - \rho_j I_j\right] \mathbf{u}_l \cdot \mathbf{c}^{ml} + \text{REAL}(\rho_j I_j)\sum_{m,l}(\mathbf{u}_l - \mathbf{u}_j)\cdot \mathbf{c}^{ml}\right\},$$

where the prime means an approximation. We use donor cell scheme (see [4]), called also UDS: we take the quantity $\rho_j I_j$ if $\mathbf{u}_l \cdot \mathbf{c}^{ml} \geq 0$ and the corresponding quantity from the other side of the face m otherwise. Here l stands for the vertex of the cell j. We also use the fact that $\sum_{m,l} \mathbf{c}^{ml} = 0$.

Various computations were realized to test the accuracy. In particularly, we assumed the double precision for all quantities and took a uniform numerical Cartesian 3D grid. Therefore, in the calculation of residuals, the maximal inaccuracy of the first order in h was only in view of UDS approximation scheme of divergence operator. Nevertheless, the time step Δt remained restricted by value h/u_{flow}. However, the suggested method is supposed not to restrict the time step by the above value h/u_{flow} and therefore Δt can be significantly increased without increase of the computation time if one uses higher order difference approximations of the spatial operators in calculation of residuals. Possibly, the reason for such a restriction of Δt may be of a more complex nature.

5. Finite-difference equations

If all the necessary quantities for the time $t^n = t$ are known, then to determine the unknown quantities for $t^{n+1} = t + \Delta t$ we use the discretized Navier–Stokes equations with a weighted scheme with the weight ω

$$\mathrm{Q}_\rho \equiv \frac{1}{\Delta t}(\rho^{n+1} - \rho^n) + \omega \operatorname{div} \rho^{n+1}\mathbf{u}^{n+1} + (1-\omega)\operatorname{div} \rho^n \mathbf{u}^n, \quad \mathrm{Q}_\rho = 0, \tag{37}$$

$$\begin{aligned}\mathbf{Q}_u \equiv{}& \frac{1}{\Delta t}(\rho^{n+1}\mathbf{u}^{n+1} - \rho^n\mathbf{u}^n) - \left[\omega\rho^{n+1} + (1-\omega)\rho^n\right]\mathbf{g} + \left[\omega\nabla p^{n+1} + (1-\omega)\nabla p^n\right] \\ &- \omega\operatorname{div}\mathbf{P}^{n+1}_{\text{visc}} - (1-\omega)\operatorname{div}\mathbf{P}^n_{\text{visc}} + \omega\operatorname{div}\rho^{n+1}\mathbf{u}^{n+1}\mathbf{u}^{n+1} + (1-\omega)\operatorname{div}\rho^n\mathbf{u}^n\mathbf{u}^n, \quad \mathbf{Q}_u = 0;\end{aligned} \tag{38}$$

$$\begin{aligned}\mathrm{Q}_I \equiv{}& \frac{1}{\Delta t}\left(\rho^{n+1}I^{n+1} - \rho^n I^n\right) - \omega\mathbf{P}^{n+1}\cdot\nabla\mathbf{u}^{n+1} - (1-\omega)\mathbf{P}^n\cdot\nabla\mathbf{u}^n - \omega\operatorname{div}\left(\frac{\lambda^{n+1}}{c_V}\nabla I^{n+1}\right) \\ &- (1-\omega)\operatorname{div}\left(\frac{\lambda^n}{c_V}\nabla I^n\right) + \omega\operatorname{div}\left(\rho^{n+1}I^{n+1}\mathbf{u}^{n+1}\right) + (1-\omega)\operatorname{div}(\rho^n I^n\mathbf{u}^n), \quad \mathrm{Q}_I = 0.\end{aligned}$$

To calculate the spatial differential operators and other terms we use the formulas in the previous section.

6. Method of solving

6.1. Principal ideas

For the initial guesses at the time $t + \Delta t$ we take the values at the time t. On every global iteration step L for the known quantities $p^{n+1}_{j,L}$, $\rho^{n+1}_{j,L}$, $I^{n+1}_{j,L}$ and $\mathbf{u}^{n+1}_{i,L}$ in all cells j and nodes i for the time $t + \Delta t$ we determine the residuals Q_ρ, Q_I in every cell j and the residuals $\mathbf{Q}_u$ in every node i. For realization the Newton-type iteration scheme and in order to avoid solving large linear systems of equations for cells j and for nodes i, let us express the variations of residuals at the iteration L as follows

$$\delta\mathrm{Q}_{\rho j} \approx \frac{\partial \mathrm{Q}_\rho}{\partial\rho}\delta\rho^{n+1}_{j,L} + \frac{\partial \mathrm{Q}_\rho}{\partial I}\delta I^{n+1}_{j,L}, \qquad \delta\mathrm{Q}_{Ij} \approx \frac{\partial \mathrm{Q}_I}{\partial\rho}\delta\rho^{n+1}_{j,L} + \frac{\partial \mathrm{Q}_I}{\partial I}\delta I^{n+1}_{j,L} \tag{39}$$

$$\delta\mathbf{Q}_{ui} \approx A_i\delta\mathbf{u}^{n+1}_{i,L}, \qquad \delta\mathbf{Q}_{uj} \approx A_j\delta\mathbf{u}^{n+1}_j. \tag{40}$$

To this end, the unknown relations between the variations of quantities at nearest cells j and j' or nodes i and i' can be replaced by artificial ones. Therefore, in the respective formulas, the following parameters appear ω_{p0}, ω_{u0}, ω_{I0}, $\omega_{\rho u0}$, ω_{puu0}.

In order to obtain the formulas for the quantities $\dfrac{\partial \mathrm{Q}_\rho}{\partial\rho}$, $\dfrac{\partial \mathrm{Q}_\rho}{\partial I}$, $\dfrac{\partial \mathrm{Q}_I}{\partial\rho}$, $\dfrac{\partial \mathrm{Q}_I}{\partial I}$ we use the variations of Q_ρ and Q_I and assume that the velocities on every iteration step are those making the momentum conservation equation to be satisfied exactly. We also assume that the variations of density, internal energy, and pressure produce a variation of velocity such that the momentum conservation equation

is satisfied exactly. Consequently, we have $\delta \mathbf{Q}_u = 0$ or the variation of residual is zero. Hence, having written the expression for the cell j instead of node i, we obtain

$$\frac{\operatorname{div} \delta(\rho_j^{n+1} \mathbf{u}_j^{n+1})}{\Delta t} = \omega \delta \operatorname{div} \rho_j^{n+1} \mathbf{g} - \omega \delta \operatorname{div} \nabla p_j^{n+1} + \omega \delta \operatorname{div} \operatorname{div} \mathbf{P}_{\text{visc},j}^{n+1} - \omega \delta \operatorname{div} \operatorname{div} (\rho_j^{n+1} \mathbf{u}_j^{n+1} \mathbf{u}_j^{n+1}).$$

After a simplification, this expression gives us a component for $\delta \mathbf{Q}_\rho$. Further simplification yields the expressions for $\delta \mathbf{Q}_\rho$, $\delta \mathbf{Q}_I$ in the form (39), where $\frac{\partial \mathbf{Q}_\rho}{\partial \rho}$, $\frac{\partial \mathbf{Q}_\rho}{\partial I}$, $\frac{\partial \mathbf{Q}_I}{\partial \rho}$, $\frac{\partial \mathbf{Q}_I}{\partial I}$ are already known quantities.

To obtain a formula for the quantity A_i we vary $\mathbf{Q}_u$ and then assume that the densities on every iteration step are those making the continuity equation to be satisfied exactly, and the variation of velocity produces the variations of density, internal energy, and pressure, which make the continuity equation to be satisfied exactly. Therefore we also have $\delta \mathbf{Q}_\rho = 0$ or the variation of residual is zero. Now, writing the expression for the node i instead of the cell j, we obtain

$$\frac{\delta \rho_i^{n+1}}{\Delta t} = -\omega \operatorname{div} \delta(\rho_i^{n+1} \mathbf{u}_i^{n+1}).$$

The latter will make it possible to connect the variations of velocity and density. Next, if we succeed to relate in any way the variations of pressure and density to each other, then this will make possible to replace in the momentum equation the variation of pressure by the variation of velocity. Further simplification gives us the expression for $\delta \mathbf{Q}_u$ at the form (40), where A_i is already known.

For optimal pressure correction iteration procedure we use discretized equations (37), (38) for the density ρ and the momentum $\rho \mathbf{u}$. These equations can be satisfied by determination of pressure p and velocity $\mathbf{u}$ and allowing p and $\mathbf{u}$ to vary only in the following terms $\operatorname{div} \rho \mathbf{u}$, $\partial \rho \mathbf{u} / \partial t$, ∇p, $\operatorname{div} \rho \mathbf{u} \mathbf{u}$. The term $\partial \rho / \partial t = (\rho^{n+1} - \rho^n)/\Delta t$ also changes in accordance with p^{n+1} in the equation of state for the fixed internal energy I^{n+1}. However, we do not vary ρ^{n+1} within such a procedure. Iterations carried out on these equations are called the Newton inner iterations. Having stopped the inner iterations, we change the density ρ^{n+1} and internal energy I^{n+1} by means of the adiabatic approximation so that their new values correspond to the new value of the pressure p^{n+1}.

The variations of residuals at the inner iteration L_p can be expressed as follows

$$\begin{aligned} \delta \mathbf{Q}_{\rho j} &\approx \frac{\partial \mathbf{Q}_\rho}{\partial p} \delta p_{j,L+1,Lp}^{n+1}, \\ \delta \mathbf{Q}_{ui} &\approx A_{ip} \delta \mathbf{u}_{i,L+1,Lp}^{n+1}. \end{aligned} \tag{41}$$

For the pressure correction method we use A_{ip} instead of A_i in correlation (40). Having simplified the term $\delta \operatorname{div} \rho \mathbf{u} \mathbf{u}$, we obtain a formula for A_{ip}. It contains the replacement parameter ω_{up0} whose sense differs from that of the above replacement parameters. We proceed with a very rough replacement $\delta(\operatorname{div} \rho \mathbf{u} \mathbf{u})_i = \omega_{up0} \sum_m |\mathbf{c}'^m| / V_i \rho u_i \delta \mathbf{u}_i$ (for the sake of simplicity, here and in some places in what follows, the index $n+1$ is omitted). For a regular hexahedron we have $V_i \Big/ \sum_m |\mathbf{c}'^m| = 0.1666h$ (in our computation we took $\omega_{up0} = 0.2$). Here V_i is the volume of a displaced cell i, $\mathbf{c}'^m$ is the geometric coefficient at the face m, h is the cube's side.

To obtain a formula for the quantity $\partial \mathbf{Q}_\rho / \partial p$ we take the variation of $\mathbf{Q}_\rho$ and assume that velocities on every iteration step are those making the discretized momentum conservation equation to be satisfied exactly, and the variation of pressure produces the variation of velocity such that the momentum equation is satisfied exactly. This makes it possible to replace $\delta \operatorname{div} \rho \mathbf{u}_j$ with the variation δp and other terms. Though we do not change the density and internal energy in the inner iterations L_p, in calculating $\mathbf{Q}_\rho$ the term $\partial \rho / \partial t = (\rho^{n+1} - \rho^n / \Delta t$ changes as $\left[\rho(p_{L+1,Lp}^{n+1}, I_{L+1}^{n+1}) - \rho^n\right] / \Delta t$ in accordance with $p_{L+1,Lp}^{n+1}$ in the state equation for the fixed internal energy I_{L+1}^{n+1} (see (49)). However, in obtaining the formula for $\partial \mathbf{Q}_\rho / \partial p$, we take into account the variation of the term $(\rho^{n+1} - \rho^n)/\Delta t$

by using the adiabatic approximation $\partial p/\partial\rho = \gamma p/\rho$. The fact is that after stopping the inner iterations we change the density and internal energy with adiabatic approximation so that their new values correspond to the new value of pressure. Further simplification results in the expressions for $\delta \mathrm{Q}_\rho$ of the form (41), where $\partial \mathrm{Q}_\rho/\partial p$ are known.

Let us give the expressions which reveal the CRCR and are derived in Sec. 7

$$\delta \mathrm{Q}_{\rho j} \approx \left[\frac{1}{\Delta t} + B_1\right] \delta\rho_j^{n+1} + B_2 \delta I_j^{n+1}, \tag{42}$$

$$\delta \mathrm{Q}_{Ij} \approx \left[\frac{I_j^{n+1}}{\Delta t} + B_1 C_3\right] \delta\rho_j^{n+1} + \left[\frac{\rho_j^{n+1}}{\Delta t} + B_2 C_3 + \omega(1-\omega_{I0}) C_1 \left(\frac{\lambda}{c_V}\right)_j^{n+1}\right] \delta I_j^{n+1}. \tag{43}$$

To reduce the calculation, we determine A_i by averaging in the volume of a displaced cell i by means of A_j. Next, A_j is obtained via the formula

$$A_j = \frac{1}{\Delta t}\rho_j^{n+1} + \omega^2 \Delta t \frac{1-\omega_{\rho u 0}}{3} C_1 \gamma(I_j^{n+1}) p_j^{n+1} + \omega \frac{7\mu(1-\omega_{u0})}{9} C_1 . \tag{44}$$

The following expressions are for the inner pressure correction iteration

$$\delta \mathrm{Q}_{\rho j} \approx \left[\frac{1}{\Delta t} + B_4 C_4\right] \frac{1}{C_4} \delta p_{j,L+1,Lp}^{n+1}, \qquad A_{ip} = \rho_i^{n+1} \left(\frac{1}{\Delta t} + \frac{\omega \omega_{up0} u_i^{n+1}}{h_6}\right). \tag{45}$$

The coefficients in the above expressions are

$$\begin{gathered}
C_1 = \frac{1}{(V_j)^2} \sum_l (\mathbf{c}^l)^2, \qquad \mathbf{c}^l = \sum_m \mathbf{c}^{ml}, \\
C_2 = (1-\omega_{p0}) \frac{p_j^{n+1}}{\rho_j^{n+1}} + (1-\omega_{\rho u u 0}) \frac{\left(u_j^{n+1}\right)^2}{3}, \qquad C_3 = I_j^{n+1} + \frac{p_j^{n+1}}{\rho_j^{n+1}}, \\
C_4 = \gamma\left(I_j^{n+1}\right) \frac{p_j^{n+1}}{\rho_j^{n+1}}, \qquad h_6 = V_i \Big/ \sum_m |\mathbf{c}'^m|, \qquad B_1 = \omega^2 \Delta t C_1 C_2, \\
B_2 = \omega^2 \Delta t (1-\omega_{p0}) \left[\gamma(I_j^{n+1}) - 1\right] \rho_j^{n+1} C_1, \qquad B_4 = (1-\omega_{p0}) \omega^2 \Delta t C_1 .
\end{gathered} \tag{46}$$

The above terms are obtained via the initial iteration guesses, i.e., in fact, the values given for time t.

6.2. Sequence of iteration cycles

We may determine increments $\delta\rho_{j,L}^{n+1}$, $\delta I_{j,L}^{n+1}$ in the Newton global iteration L

$$\delta\rho_L^{n+1} = -\frac{\mathrm{Q}_\rho\left(\rho_L^{n+1}, I_L^{n+1}, p_L^{n+1}, \mathbf{u}_L^{n+1}\right) \partial \mathrm{Q}_I/\partial I^{n+1} - \mathrm{Q}_I\left(\rho_L^{n+1}, I_L^{n+1}, p_L^{n+1}, \mathbf{u}_L^{n+1}\right) \partial \mathrm{Q}_\rho/\partial I^{n+1}}{D_{\mathrm{Q}}},$$

$$\delta I_L^{n+1} = -\frac{\mathrm{Q}_I\left(\rho_L^{n+1}, I_L^{n+1}, p_L^{n+1}, \mathbf{u}_L^{n+1}\right) \partial \mathrm{Q}_\rho/\partial \rho^{n+1} - \mathrm{Q}_\rho\left(\rho_L^{n+1}, I_L^{n+1}, p_L^{n+1}, \mathbf{u}_L^{n+1}\right) \partial \mathrm{Q}_I/\partial \rho^{n+1}}{D_{\mathrm{Q}}}.$$

One can easily verify that the discriminant D_{Q}

$$D_{\mathrm{Q}} = \frac{\partial \mathrm{Q}_\rho}{\partial\rho}\frac{\partial \mathrm{Q}_I}{\partial I} - \frac{\partial \mathrm{Q}_I}{\partial\rho}\frac{\partial \mathrm{Q}_\rho}{\partial I},$$

always exceeds zero. Then

$$\rho_{j,L+1}^{n+1} = \rho_{j,L}^{n+1} + \omega_\rho \delta\rho_{j,L}^{n+1}\,,$$
$$I_{j,L+1}^{n+1} = I_{j,L}^{n+1} + \omega_I \delta I_{j,L}^{n+1}\,. \tag{47}$$

Here to the relaxation parameter ω_L (which is ω_ρ for density and ω_I for energy) we assigned the value 1. By determining $p_{j,L+1}^{n+1}$ in the state equation, we find $\mathbf{u}_{i,L+1}^{n+1}$ via the equations

$$A_i \delta\mathbf{u}_{i,L}^{n+1} = -\mathbf{Q}_{ui}\left(\rho_{L+1}^{n+1}, I_{L+1}^{n+1}, p_{L+1}^{n+1}, \mathbf{u}_L^{n+1}\right),$$
$$\mathbf{u}_{i,L+1}^{n+1} = \mathbf{u}_{i,L}^{n+1} + \delta\mathbf{u}_{i,L}^{n+1}. \tag{48}$$

Next, if we introduce the pressure correction iteration procedure, this does not increase the time step. Therefore, we do not use (47) and will not change the pressure p. Instead of this we determine $\rho_{j,L+1}^{n+1}$ from the state equation via $I_{j,L+1}^{n+1}$ and $p_{j,L+1}^{n+1} = p_{j,L}^{n+1}$. We then determine $\mathbf{u}_{i,L+1}^{n+1}$ from Eqs. (48). Now we pass to introducing the pressure correction procedure into the inner iterations. In the inner iteration L_p the corrected values of pressure are determined from the equations

$$\delta p_{L+1,Lp}^{n+1} = -\frac{\mathbf{Q}_\rho\left(\rho(p_{L+1,Lp}^{n+1}, I_{L+1}^{n+1}),\ I_{L+1}^{n+1},\ p_{L+1,Lp}^{n+1},\ \mathbf{u}_{L+1,Lp}^{n+1}\right)}{\partial\mathbf{Q}_\rho/\partial p^{n+1}},$$
$$p_{j,L+1,Lp+1}^{n+1} = p_{j,L+1,Lp}^{n+1} + \omega_p \delta p_{j,L+1,Lp}^{n+1}. \tag{49}$$

Here $\rho(p_{L+1,Lp}^{n+1}, I_{L+1}^{n+1})$ expresses the state equation and is used only for computation of term $\partial\rho/\partial t = (\rho^{n+1} - \rho^n)/\Delta t$ (in our computation the relaxation parameter ω_p was assumed to be equal to 1). Afterwards we determine $\mathbf{u}_{i,L+1}^{n+1}$ via the equations

$$A_{ip}\delta\mathbf{u}_{i,L+1,Lp}^{n+1} = -\mathbf{Q}_{ui}\left(\rho_{L+1}^{n+1}, I_{L+1}^{n+1}, p_{L+1,Lp+1}^{n+1}, \mathbf{u}_{L+1,Lp}^{n+1}\right),$$
$$\mathbf{u}_{i,L+1,Lp+1}^{n+1} = \mathbf{u}_{i,L+1,Lp}^{n+1} + \delta\mathbf{u}_{i,L+1,Lp}^{n+1}.$$

Further, let us describe the proper sequence of iterations. We start the global and inner iterations with $L = 0$, $L_p = 0$. We restrict the inner iteration L_p by the limits for $L_p + 1$ from 2 to 5. If the $L_p + 1 \geq 2$ and

$$\delta_{u(P-\text{link})} = \max\left(|\delta u| + |\delta v| + |\delta w|\right)/|\mathbf{u}_{\max}| < \varepsilon_{u(P-\text{link})}\,,$$

or $L_p + 1 = 5$, then we stop the inner iteration L_p. Otherwise we move to the next iteration $L_p + 1$. After stopping inner pressure correction iterations we change the density and internal energy by means adiabatic approximation so that new values of them correspond to new value of pressure with the state equation. Then we go to the next global iteration $L + 1$.

We restrict the global iteration L by the limits from 2 to 15 for $L + 1$. If the $L + 1 \geq 2$ and

$$\delta_{\rho,I} = \max|\delta\rho|/\rho_{\max} + \max|\delta I|/I_{\max} < \varepsilon_{\rho,I}\,, \tag{50}$$
$$\delta_u = \max\left(|\delta u| + |\delta v| + |\delta w|\right)/|\mathbf{u}_{\max}| < \varepsilon_u\,, \tag{51}$$

and for the last inner iteration of preceding global iteration we have

$$\delta_{u(P-\text{link})} = \max\left(|\delta u| + |\delta v| + |\delta w|\right)/|\mathbf{u}_{\max}| < \varepsilon_{u(P-\text{link})}\,, \tag{52}$$

or $L + 1 = 15$, then we stop the global iteration L. Otherwise we go to the first $L_p = 0$ inner iteration. After a catastrophic stop of the global iterations (if $L + 1 = 15$) we sharply decrease the time step $\Delta t_{\text{new}} = 0.75\Delta t_{\text{old}}$ and begin the iteration process again with the same t. After a regular stop of the global iterations (if $L + 1 < 15$) in accordance with the convergence criteria (50)–(52), we pass to the next time $t + \Delta t_{\text{new}}$ and change the time step in accordance with the sum of the three last numbers of the preceding global iterations, i.e., $\Delta t_{\text{new}} = 0.9\Delta t_{\text{old}}$ if the sum exceeds 13, $\Delta t_{\text{new}} = 1.01\Delta t_{\text{old}}$ if the sum is lesser than 10. The previous choice establishes the number of global iterations equal to 4 on average as well as the corresponding value of the time step.

6.3. Convergence criteria

In our low Mach number flow testing tasks we took: $\varepsilon_{\rho,I} = 2 \cdot 10^{-5}$, $\varepsilon_u = 0.3 \cdot 10^{-5}$, $\varepsilon_{u(P-\text{link})} = 0.2 \cdot 10^{-3}$. The convergence criterion for the velocity in the pressure correction inner iterations is more rough than the criterion in the global iterations, because with $\Delta t \approx h/u_{\text{flow}}$ and the low Mach number flow, we have $A_{ip} \ll A_i$ and therefore $\delta\mathbf{u} \ll \delta\mathbf{u}_{(P-\text{link})}$. The velocity correction in the global iteration can be thus considered as a more fine than that in the pressure correction inner iterations.

7. Obtaining formulas for CRCR

To deduce the formulas for CRCR we should obtain an approximate correlation between the variations of residuals $\delta\mathrm{Q}_\rho$, $\delta\mathrm{Q}_I$, and $\delta\rho$, δI and between the variations of residuals $\delta\mathbf{Q}_u$ and $\delta\mathbf{u}$.

First of all we find the variation of $\mathbf{Q}_u$ in the node i

$$\delta\mathbf{Q}_u = \frac{1}{\Delta t}\left(\rho_i^{n+1}\delta\mathbf{u}_i^{n+1} + \mathbf{u}_i^{n+1}\delta\rho_i^{n+1}\right) - \omega\delta\rho_i^{n+1}\mathbf{g} + \omega\delta\nabla p_i^{n+1} - \omega\delta\,\mathrm{div}\,\mathbf{P}_{\text{visc},i}^{n+1} + \omega\delta\,\mathrm{div}\left(\rho_i^{n+1}\mathbf{u}_i^{n+1}\mathbf{u}_i^{n+1}\right). \tag{53}$$

For a displaced cell around the node i, from formula (30) or (36) we obtain

$$\mathrm{div}\,\mathbf{P}_{\text{visc},i}^{n+1} = \frac{1}{V_i}\sum_l \mathbf{c}'^l \cdot \mathbf{P}_{\text{visc},l}^{n+1}. \tag{54}$$

Here V_i is the volume of the displaced cell (we omit prime here). Figure 6 shows the location of indexes. In the centre of this scheme the displaced cell i (shown by dotting) has the vertices l which are the centroids of the usual cells l around the node i. The vertices of the cell l are the nodes i' which may coincide with the node i. In the left lower part of scheme the indexes l obtain a slightly different sense. The usual cell j has the vertices l which are the centroids of the displaced cells l around the node j. The vertices of the displaced cell l are the centroids j' of the cells j' which may coincide with the centroid j.

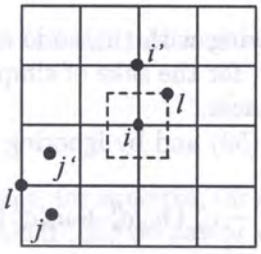

Fig. 6. The location of indexes

By introducing the new indexes m, e, and s (they are equal to 1,2,3, respectively, for the rectangular coordinates x, y, z), from Eq. (2) we have

$$\left(\mathbf{P}_{\text{visc},l}^{n+1}\right)_{e,s} = -\frac{1}{3}\mu e_{mml}\delta_{es} + \mu e_{esl}, \tag{55}$$

$$\mathrm{div}\,\mathbf{P}_{\text{visc},i}^{n+1}\Big|_1 = \frac{1}{V_i}\sum_{esl}\mu e_{esl}\mathbf{c}'^l \cdot \mathbf{i}_e\mathbf{i}_s\,; \qquad \mathrm{div}\,\mathbf{P}_{\text{visc},i}^{n+1}\Big|_2 = -\frac{1}{3V_i}\sum_{esl}\mu e_{mml}\delta_{es}\mathbf{c}'^l \cdot \mathbf{i}_e\mathbf{i}_s\,. \tag{56}$$

Here e_{esl} is a component of the strain velocity tensor at the point (cell) l, the repeated index m means the summation over the index m, and the unit vector $\mathbf{i}_e$ is as follows

$$\mathbf{i}_e = \begin{cases} \mathbf{i}, & \text{for} \quad e = 1, \\ \mathbf{j}, & \text{for} \quad e = 2, \\ \mathbf{k}, & \text{for} \quad e = 3. \end{cases}$$

Equation (3) implies

$$e_{esl} = \frac{\partial u_e}{\partial x_s}\bigg|_l + \frac{\partial u_s}{\partial x_e}\bigg|_l = \frac{1}{V_l}\sum_{i'}\left(u_{ei'}c_s^{i'} + u_{si'}c_e^{i'}\right)$$

$$\sum_l e_{esl}\mathbf{c}'^l \cdot \mathbf{i}_e\mathbf{i}_s = \sum_l \frac{1}{V_l}\mathbf{c}'^l \cdot \mathbf{i}_e\mathbf{i}_s \sum_{i'}\left(u_{ei'}c_s^{i'} + u_{si'}c_e^{i'}\right) = \mathbf{i}_s \sum_l \frac{1}{V_l}c_e'^l \sum_{i'}\left(u_{ei'}c_s^{i'} + u_{si'}c_e^{i'}\right)$$

$$= \mathbf{i}_s \sum_l \frac{1}{V_l}c_e'^l \left(u_{ei}c_s^i + \sum_{i'\neq i} u_{ei'}c_s^{i'} + u_{si}c_e^i + \sum_{i'\neq i} u_{si'}c_e^{i'}\right). \tag{57}$$

The correlation (23) for coefficients $\mathbf{c}$ yields

$$\sum_{i'\neq i}\mathbf{c}^{i'} = -\mathbf{c}^i.$$

The coefficients $\mathbf{c}$ and $\mathbf{c}'$ of the usual and good displaced cells correlate approximately as follows:

$$\mathbf{c}^i \approx -\mathbf{c}'^l.$$

Then from the above formulas it follows

$$c_s^i \approx -c_s'^l, \qquad c_e^i \approx -c_e'^l, \qquad \sum_{i'\neq i} c_s^{i'} = -c_s^i, \qquad \sum_{i'\neq i} c_e^{i'} = -c_e^i. \tag{58}$$

Assume that the velocities at node i and i' correlate approximately as follows

$$\mathbf{u}_{i'} \approx \omega_{u0}(i, i')\mathbf{u}_i, \tag{59}$$

where i' stands for the nodes neighbouring with the node i. Certainly, this correlation takes place for the variations of velocities; however, for the sake of simplicity, we will omit the variation sign δ at quantities here and in some other places.

From (57) with regard for (58) and (59) and by ignoring that ω_{u0} depends on i', we obtain

$$\sum_l e_{esl}\mathbf{c}'^l \cdot \mathbf{i}_e\mathbf{i}_s \approx -\mathbf{i}_s(1-\omega_{u0})\sum_l \frac{1}{V_l}c_e'^l\left(u_{ei}c_s'^l + u_{si}c_e'^l\right).$$

Taking the sum in the last equation over the indexes e and s and ignoring the dependence of μ on l, from (56) we have

$$\operatorname{div}\mathbf{P}^{n+1}_{\text{visc},\,i}\Big|_1 \approx \frac{\mu(1-\omega_{u0})}{V_i}\sum_{esl}\left[-\mathbf{i}_s\frac{1}{V_l}c_e'^l\left(u_{ei}c_s'^l + u_{si}c_e'^l\right)\right]. \tag{60}$$

Correlation (23) for coefficients $\mathbf{c}'$ implies

$$\sum_l \mathbf{i}_s c_s'^l = 0, \qquad \sum_l \mathbf{c}'^l = 0, \qquad \sum_e (c_e'^l)^2 = (\mathbf{c}'^l)^2.$$

From the last relations and (60) for the term in Eq. (53) it follows

$$\delta \operatorname{div} \mathbf{P}^{n+1}_{\text{visc},i}\Big|_1 \approx -\delta \mathbf{u}_i \mu \frac{(1-\omega_{u0})}{V_i} \sum_l (\mathbf{c}'^l)^2/V_l\,. \tag{61}$$

Indeed, in (61) not only the component with $\delta\mathbf{u}_i$ must stay but also others perpendicular to the first one. We have derived this primitive correlation because we used (59). In a similar way, from (56) and introducing explicitly the sum for repeating index m, we obtain

$$\begin{aligned}
\operatorname{div} \mathbf{P}^{n+1}_{\text{visc},i}\Big|_2 &= -\frac{\mu}{3V_i} \sum_{mesl} e_{mml}\delta_{es}\mathbf{c}'^l \cdot \mathbf{i}_e\mathbf{i}_s = -\frac{\mu}{3V_i} \sum_{mel} e_{mml}c'^l_e\mathbf{i}_e = -\frac{2\mu}{3V_i} \sum_l \operatorname{div}(\mathbf{u}_l)\mathbf{c}'^l \\
&= -\frac{2\mu}{3V_i} \sum_l \frac{1}{V_l} \sum_{i'} \mathbf{u}_{i'} \cdot \mathbf{c}^{i'}\mathbf{c}'^l = -\frac{2\mu}{3V_i} \sum_l \frac{1}{V_l} \left(\mathbf{u}_i \cdot \mathbf{c}^i + \sum_{i' \neq i} \mathbf{u}_{i'} \cdot \mathbf{c}^{i'} \right) \mathbf{c}'^l \\
&\approx -\frac{2\mu}{3V_i} \sum_l \frac{1}{V_l} (1-\omega_{u0}) \mathbf{u}_i \cdot \mathbf{c}^i\mathbf{c}'^l = \frac{2\mu(1-\omega_{u0})}{3V_i} \mathbf{u}_i \cdot \sum_l \mathbf{c}'^l\mathbf{c}'^l \Big/ V_l\,.
\end{aligned} \tag{62}$$

Let us obtain the approximate correlation for $\mathbf{u} \cdot \sum_l \mathbf{c}^l\mathbf{c}^l/V_l$. For the sake of convenience, we omit for now the primes at the geometric coefficients and index i. Let

$$\mathbf{u} = \mathbf{u}_{c^l} + \mathbf{u}^1_{\perp c^l} + \mathbf{u}^2_{\perp c^l}\,, \tag{63}$$

where the first summand is the component of $\mathbf{u}$ along the direction of $\mathbf{c}^l$, the two other summands are components perpendicular to the direction of $\mathbf{c}^l$, i.e., along the directions of $\overset{1}{\perp}\mathbf{c}^l$ and $\overset{2}{\perp}\mathbf{c}^l$, which are independent of $\mathbf{u}$ and are defined in a certain manner by the vector $\mathbf{c}^l$. Consequently,

$$\mathbf{u} \cdot \sum_l \mathbf{c}^l\mathbf{c}^l/V_l = \sum_l u_{c^l}c^l\mathbf{c}^l/V_l = \sum_l \mathbf{u}_{c^l}(\mathbf{c}^l)^2/V_l\,. \tag{64}$$

Since in the sum over l the coefficients $\mathbf{c}^l$ may have different directions, by the symmetry we may assume

$$\sum_l \mathbf{u}_{c^l}(c^l)^2/V_l \approx \sum_l \mathbf{u}^1_{\perp c^l}(\mathbf{c}^l)^2/V_l \approx \sum_l \mathbf{u}^2_{\perp c^l}(\mathbf{c}^l)^2/V_l\,.$$

Summation of all the three members in the last relations with regard for (63) and (64) implies

$$\mathbf{u} \cdot \sum_l \mathbf{c}^l\mathbf{c}^l/V_l \approx \mathbf{u} \sum_l (\mathbf{c}^l)^2/3V_l\,, \tag{65}$$

as was necessary. For regular polyhedrons, for example, for a cube or a tetrahedron, this correlation turns to be exact. Therefore from (62) and (65) we have

$$\delta \operatorname{div} \mathbf{P}^{n+1}_{\text{visc},i}\Big|_2 \approx \delta \mathbf{u}_i \frac{2\mu}{9} \frac{(1-\omega_{u0})}{V_i} \sum_l (c'^l)^2/V_l\,,$$

and from the latter, by taking into account (61), by Eqs. (54)–(56) we have

$$\delta \operatorname{div} \mathbf{P}^{n+1}_{\text{visc},i} \approx -\delta \mathbf{u}_i \frac{7\mu}{9} \frac{(1-\omega_{u0})}{V_i} \sum_l (\mathbf{c}'^l)^2/V_l\,. \tag{66}$$

The last formula has a simple physical interpretation. From both the momentum equation (38) and (66) it follows that the variation of velocity generates an opposite braking force.

Let us turn to $\delta \mathrm{Q}_\rho$. From (37) we obtain

$$\delta \mathrm{Q}_\rho = \frac{\delta \rho_j^{n+1}}{\Delta t} + \omega \operatorname{div} \delta \left(\rho_j^{n+1} \mathbf{u}_j^{n+1} \right). \tag{67}$$

The second term is obtained by means of the divergence of the momentum equation. In the determination of the variations of density, internal energy, and pressure, it is assumed that the velocities on every iteration step make the momentum equation to be satisfied exactly, and the variations of density, internal energy, and pressure produce the variation of velocity such that the momentum equation is satisfied exactly. Consequently, we have $\delta \mathbf{Q}_u = 0$ or the variation of residual is zero. Now from (53), by writing the expression for the cell j instead of node i, we obtain

$$\begin{aligned} \frac{\operatorname{div} \delta \left(\rho_j^{n+1} \mathbf{u}_j^{n+1} \right)}{\Delta t} &= \omega \delta \operatorname{div} \rho_j^{n+1} \mathbf{g} - \omega \delta \operatorname{div} \nabla p_j^{n+1} \\ &\quad + \omega \delta \operatorname{div} \operatorname{div} \mathbf{P}_{\mathrm{visc},j}^{n+1} - \omega \delta \operatorname{div} \operatorname{div} \left(\rho_j^{n+1} \mathbf{u}_j^{n+1} \mathbf{u}_j^{n+1} \right). \end{aligned} \tag{68}$$

The next formulas will be obtained in a way analogous to that for the variation of the divergence of $\mathbf{P}_{\mathrm{visc}}$. As above, for the sake of simplicity, we omit the variation sign δ at variables.

We denote by ω_{p0} the derivative of pressure at the cell j' with respect to the pressure at the cell j

$$\omega_{p0} = \partial p_{j'}^{n+1} / \partial p_j^{n+1};$$

here we omit the indexes in the first term, j' stands for cells neighbouring with the cell j. We have

$$\begin{aligned} \operatorname{div} \nabla p_j &= \frac{1}{V_j} \sum_l \nabla p_l \cdot \mathbf{c}^l = \frac{1}{V_j} \sum_l \frac{1}{V_l} \left(p_j \mathbf{c}'^j + \sum_{j' \neq j} p_{j'} \mathbf{c}'^{j'} \right) \cdot \mathbf{c}^l \\ &\approx \frac{1}{V_j} \sum_l \frac{1}{V_l} \left(p_j \mathbf{c}'^j + p_j \sum_{j' \neq j} \omega_{p0}(j, j') \mathbf{c}'^{j'} \right) \cdot \mathbf{c}^l \approx p_j \frac{1 - \omega_{p0}}{V_j} \sum_l \frac{1}{V_l} \mathbf{c}'^j \cdot \mathbf{c}^l, \\ \delta \operatorname{div} \nabla p_j &\approx -\delta p_j \frac{1 - \omega_{p0}}{V_j} \sum_l (\mathbf{c}^l)^2 / V_l \approx -\delta p_j \frac{1 - \omega_{p0}}{(V_j)^2} \sum_l (\mathbf{c}^l)^2. \end{aligned} \tag{69}$$

The term $\sum_l (\mathbf{c}^l)^2 / (V_j)^2$ by its value is equivalent to $1h^2$.

Let us determine the approximation for $\operatorname{div} \operatorname{div}(\rho_j \mathbf{u}_j \mathbf{u}_j)$ in (68):

$$\begin{aligned} \operatorname{div} \operatorname{div}(\rho_j \mathbf{u}_j \mathbf{u}_j) &= \frac{1}{V_j} \sum_l \mathbf{c}^l \cdot \operatorname{div} \rho_l \mathbf{u}_l \mathbf{u}_l = \frac{1}{V_j} \sum_l \frac{1}{V_l} \mathbf{c}^l \cdot \sum_{j'} \rho_{j'} \mathbf{c}'^{j'} \cdot \mathbf{u}_{j'} \mathbf{u}_{j'} \\ &\approx \frac{1}{V_j} \sum_l \frac{1}{V_l} \left(\rho_j \mathbf{c}'^j \cdot \mathbf{u}_j \mathbf{u}_j + \sum_{j' \neq j} \rho_{j'} \mathbf{c}'^{j'} \cdot \mathbf{u}_{j'} \mathbf{u}_{j'} \right) \cdot \mathbf{c}^l, \\ \sum_{j' \neq j} \rho_{j'} \mathbf{c}'^{j'} \cdot \mathbf{u}_{j'} \mathbf{u}_{j'} &\approx \omega_{\rho u u 0} \rho_j \mathbf{u}_j \mathbf{u}_j \sum_{j' \neq j} \cdot \mathbf{c}'^{j'} = -\omega_{\rho u u 0} \rho_j \mathbf{u}_j \mathbf{u}_j \cdot \mathbf{c}'^j. \end{aligned}$$

Thus, taking into account (65), we have

$$\begin{aligned} \operatorname{div} \operatorname{div}(\rho_j \mathbf{u}_j \mathbf{u}_j) &\approx \frac{1}{V_j} \sum_l \frac{1 - \omega_{\rho u u 0}}{V_l} \left(\rho_j \mathbf{u}_j \mathbf{u}_j \cdot \mathbf{c}'^j \right) \cdot \mathbf{c}^l \approx -\frac{1 - \omega_{\rho u u 0}}{V_j} \sum_l \frac{1}{V_l} (\rho_j \mathbf{u}_j \mathbf{u}_j \cdot \mathbf{c}^l) \cdot \mathbf{c}^l \\ &\approx -\frac{1 - \omega_{\rho u u 0}}{V_j} \rho_j \mathbf{u}_j \cdot \left(\mathbf{u}_j \cdot \sum_l \mathbf{c}^l \mathbf{c}^l / V_l \right) \approx -\frac{1 - \omega_{\rho u u 0}}{3 (V_j)^2} \rho_j u_j^2 \sum_l (\mathbf{c}^l)^2. \end{aligned}$$

The latter implies

$$\delta \operatorname{div}\operatorname{div}(\rho_j \mathbf{u}_j \mathbf{u}_j) \approx -\delta\rho_j \frac{1-\omega_{\rho uu0}}{3V_j} u_j^2 \sum_l (\mathbf{c}^l)^2/V_l - 2u_j \delta u_j \frac{1-\omega_{\rho uu0}}{3V_j} \rho_j \sum_l (\mathbf{c}^l)^2/V_l .$$

Let us transform (68), taking into account (69), the last equation, and rewriting (66) for the cell j instead of the node i:

$$\begin{aligned}
\operatorname{div}\delta(\rho_j^{n+1}\mathbf{u}_j^{n+1}) &= \omega\Delta t\delta \operatorname{div}\rho_j^{n+1}\mathbf{g} - \omega\Delta t\delta \operatorname{div}\nabla p_j^{n+1} + \omega\Delta t\delta \operatorname{div}\operatorname{div}\mathbf{P}_{\text{visc},j}^{n+1} \\
&\quad - \omega\Delta t\delta \operatorname{div}\operatorname{div}(\rho_j^{n+1}\mathbf{u}_j^{n+1}\mathbf{u}_j^{n+1}) \approx \omega\Delta t\delta \operatorname{div}\rho_j^{n+1}\mathbf{g} \\
&\quad + \omega\Delta t\delta p_j^{n+1} \frac{1-\omega_{p0}}{(V_j)^2} \sum_l (\mathbf{c}^l)^2 - \omega\Delta t \operatorname{div}(\delta\mathbf{u}_j^{n+1}) \frac{7\mu}{9} \frac{(1-\omega_{u0})}{(V_j)^2} \sum_l (\mathbf{c}^l)^2 \\
&\quad + \omega\Delta t\delta\rho_j^{n+1} \frac{1-\omega_{\rho uu0}}{3(V_j)^2} (u_j^{n+1})^2 \sum_l (\mathbf{c}^l)^2 \\
&\quad + \omega\Delta t\, 2u_j^{n+1}\delta u_j^{n+1} \frac{1-\omega_{\rho uu0}}{3(V_j)^2} \rho_j \sum_l (\mathbf{c}^l)^2 .
\end{aligned} \tag{70}$$

By substituting (70) into (67), we obtain

$$\begin{aligned}
\delta \mathrm{Q}_\rho &\approx \frac{\delta\rho_j^{n+1}}{\Delta t} + \omega^2\Delta t\delta \operatorname{div}\rho_j^{n+1}\mathbf{g} + \omega^2\Delta t\,\delta p_j^{n+1} \frac{1-\omega_{p0}}{(V_j)^2} \sum_l (\mathbf{c}^l)^2 \\
&\quad + \omega^2\Delta t\,\delta\rho_j^{n+1} \frac{1-\omega_{\rho uu0}}{3(V_j)^2} (u_j^{n+1})^2 \sum_l (\mathbf{c}^l)^2 - \omega^2\Delta t \operatorname{div}(\delta\mathbf{u}_j^{n+1}) \frac{7\mu}{9} \frac{(1-\omega_{u0})}{(V_j)^2} \sum_l (\mathbf{c}^l)^2 \\
&\quad + \omega^2\Delta t\, 2u_j^{n+1}\delta u_j^{n+1} \frac{1-\omega_{\rho uu0}}{3(V_j)^2} \rho_j^{n+1} \sum_l (\mathbf{c}^l)^2 .
\end{aligned} \tag{71}$$

We could need an expression for $\operatorname{div}\delta\mathbf{u}_j$ and $\delta\mathbf{u}_j$; however, it is not necessary to determine $\delta\mathbf{u}_j$ if in (71) and (70) we neglect the last term after comparison with a term containing δp. Next, in (70), we omit some terms of arbitrary signs. In the left-hand side, by factoring out the density at both the divergence and variation operators, we obtain

$$\begin{aligned}
\rho_j \operatorname{div}\delta\mathbf{u}_j &\approx \omega\Delta t\,\delta p_j \frac{1-\omega_{p0}}{(V_j)^2} \sum_l (\mathbf{c}^l)^2 - \omega\Delta t \operatorname{div}(\delta\mathbf{u}_j) \frac{7\mu}{9} \frac{(1-\omega_{u0})}{(V_j)^2} \sum_l (\mathbf{c}^l)^2 \\
&\quad + \omega\Delta t\delta\rho_j \frac{1-\omega_{\rho uu0}}{3(V_j)^2} u_j^2 \sum_l (\mathbf{c}^l)^2 .
\end{aligned}$$

Hence we have

$$\begin{aligned}
\operatorname{div}\delta\mathbf{u}_j \approx &\left[\omega\,\delta p_j \frac{1-\omega_{p0}}{(V_j)^2} \sum_l (\mathbf{c}^l)^2 + \omega\delta\rho_j \frac{1-\omega_{\rho uu0}}{3(V_j)^2} u_j^2 \sum_l (\mathbf{c}^l)^2\right] \\
&\cdot \left[\frac{\rho_j}{\Delta t} + \omega \frac{7\mu}{9} \frac{(1-\omega_{u0})}{(V_j)^2} \sum_l (\mathbf{c}^l)^2\right]^{-1} .
\end{aligned} \tag{72}$$

From (71), by omitting the last term and some terms of arbitrary signs, after substituting (72) into (71), we obtain

$$\delta Q_\rho \approx \frac{\delta\rho_j^{n+1}}{\Delta t} + \omega^2 \Delta t\, \delta p_j^{n+1} \frac{1-\omega_{p0}}{(V_j)^2} \sum_l (\mathbf{c}^l)^2 + \omega^2 \Delta t\, \delta\rho_j^{n+1} \frac{1-\omega_{\rho uu0}}{3(V_j)^2} (u_j^{n+1})^2 \sum_l (\mathbf{c}^l)^2$$
$$- \omega^2 \Delta t \frac{7\mu}{9} \frac{(1-\omega_{u0})}{(V_j)^2} \sum_l (\mathbf{c}^l)^2 \cdot \left[\frac{\rho_j^{n+1}}{\Delta t} + \omega \frac{7\mu}{9} \frac{(1-\omega_{u0})}{(V_j)^2} \sum_l (\mathbf{c}^l)^2 \right]^{-1}$$
$$\cdot \left[\omega \delta p_j^{n+1} \frac{1-\omega_{p0}}{(V_j)^2} \sum_l (\mathbf{c}^l)^2 + \omega \delta\rho_j^{n+1} \frac{1-\omega_{\rho uu0}}{3(V_j)^2} (u_j^{n+1})^2 \sum_l (\mathbf{c}^l)^2 \right].$$

It is clear that the sign of the last member at the variations of pressure and density is negative, because the change of velocity caused by pressure and density decrease due to the viscosity. We neglect the last term in order to increase the rate of change of the residual, which can be finally determined in the following relation

$$\delta Q_\rho \approx \frac{\delta\rho_j^{n+1}}{\Delta t} + \omega^2 \Delta t \delta p_j^{n+1} \frac{1-\omega_{p0}}{(V_j)^2} \sum_l (\mathbf{c}^l)^2 + \omega^2 \Delta t \delta\rho_j^{n+1} \frac{1-\omega_{\rho uu0}}{3(V_j)^2} (u_j^{n+1})^2 \sum_l (\mathbf{c}^l)^2. \tag{73}$$

Take logarithm of (1) and then vary it. Using (4) we obtain

$$\delta p = \frac{p}{\rho} \delta\rho + [\gamma(I) - 1]\rho \delta I.$$

From the last equation and (73) formula (42) follows.

In a similar way all formulas (43)–(46) which reveal the CRCR can be obtained.

8. Testing of the method and example of computation

We present some results on modelling for a heated viscous gas flow (argon) in a tube of an electrothermal vaporization (ETV) system. This problem was used for both testing and deriving of an effective numerical method. It also helped us to formulate the final version of the formulas of CRCR in the Newton global iteration procedure and the Newton inner pressure correction iteration procedure. The chosen values of tube length and regime of heating only simulate a real process. To reduce the calculation we consider the axial symmetry case; however, since the program is designed for the 3D calculation, the 3D cells are constructed. Let us note that the region of tube is not filled completely. The scalar quantities in symmetric cells and nodes were taken from the ordinary cells and nodes, and the vector quantities are defined from the ordinary nodes by rotating around the axis of symmetry. The fragment of used mesh has been already given in Fig. 1. Figure 7 illustrates the scheme of the tube and faces of cells in longitudinal and radial planes. For the sake of convenience, we restore the whole domain of longitudinal section of the tube from the calculated axial symmetry part. The tube radius a in the narrow part is equal to 3 mm. The heating tube walls are drawn in black.

The wall temperature $T_w(x,t)$ in ETV depends on both the longitudinal coordinate x and the time t. The temperature $T_w(0,t)$ at the tube's centre was taken from [7] and it is shown in Fig. 8. It increases from $T_0 = 300$ K to 450K within the time t passing from 11s to 12s; afterwards it rises from 450 K to 2750 K for the time t changing from 22 s to 23 s, then it decreases from 2750 K to T_0 for the time t increasing from 28 s to 39 s. The following spatial dependence of the wall temperature was given for x in mm

$$\begin{aligned} &\text{for } |x| > 16.8 \quad T_w(x,t) = T_0 = 300 \text{ K}, \\ &\text{for } 14 < |x| \le 16.8 \quad T_w(x,t) = \frac{16.8 - |x|}{2.8} \max[T_0, T_w(0,t)/2] + \frac{|x| - 14}{2.8} T_0, \end{aligned} \tag{74}$$

which constitutes a linear interpolation.

$$\text{for } |x| \le 14 \quad T_w(x,t) = \max\left[T_0,\, T_w(0,t)(1/2)^{(x/14)^2}\right]. \tag{75}$$

This equation contains a Gaussian distribution described in [8] as the closest fitting to experimental dependence.

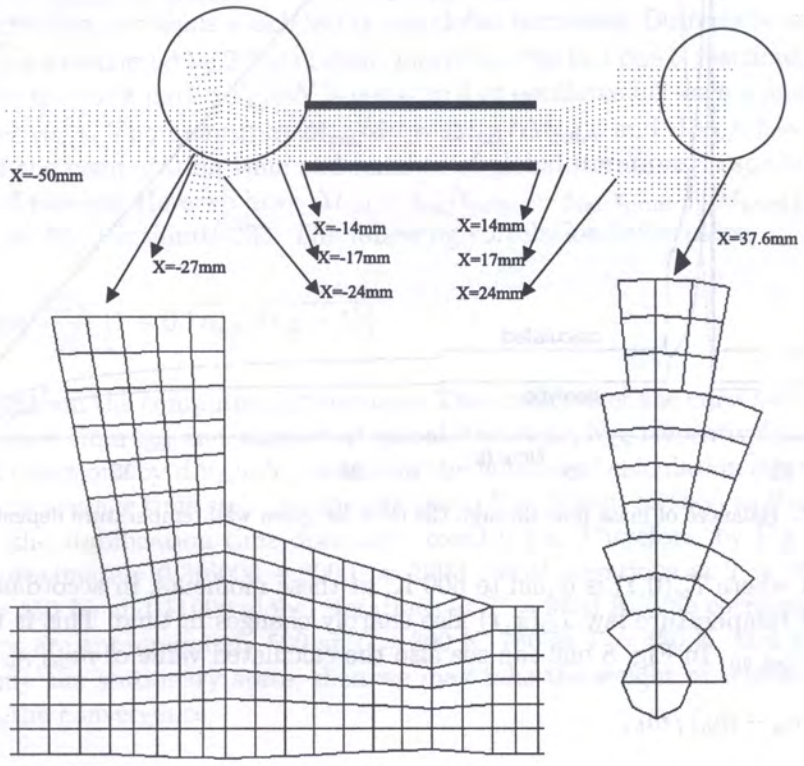

Fig. 7. The scheme of the tube and the faces of cells in the longitudinal and radial planes

To determine the change in volume with respect to the time, in [7] the simplistic model was suggested which includes: 1) the gas temperature inherits the wall temperature at any given time t and position x in the system, and 2) the pressure in the system is assumed to be constant. In a similar way, we obtain an analytic formula for the mass flow balance. Let the coordinates of tube ends be x_a and x_b, the output and input volume flow through the ends be Q_a and $\mathrm{Q}_b = \mathrm{Q}_{\mathrm{inp}}$, respectively, the output and input mass flow through the ends be $m_a = \rho_a \mathrm{Q}_a$ and $m_b = \rho_b \mathrm{Q}_b$, respectively. Assume that the cross-section area is $A(x)$ and the mass of gas in the region $[x_a,\, x_b]$ is M. For the input flow we have $\rho_b = \rho_0$ which is the density at $T_0 = 300$ K. Therefore

$$M = \int_{x_a}^{x_b} \rho A(x)\,\mathrm{d}x = \frac{p}{R}\int_{x_a}^{x_b} \frac{A(x)\,\mathrm{d}x}{T_w(x,t)}.$$

In accordance with the temperature law (74)–(75), the analytic expression for the balance of mass flow through the ends with respect to the input mass flow $m_{\mathrm{bal,an}}$ is

$$m_{\mathrm{bal,\,an}} = -\frac{\mathrm{d}M}{\mathrm{d}t}\Big/ m_b = -\frac{2\pi a^2}{\mathrm{Q}_{\mathrm{inp}}}\int_0^{16.8} \frac{\mathrm{d}}{\mathrm{d}t}\left(\frac{T_0}{T_w(x,t)}\right)\mathrm{d}x.$$

The time-dependent profile of $m_{\mathrm{bal,an}}$ for the input volume flow $\mathrm{Q}_{\mathrm{inp}} = 900$ ml/min is given in Fig. 8. In addition to evident sharp changes of $m_{\mathrm{bal,an}}$ at $t = 11$ s, 12 s, 22 s, 23 s, 28 s, 39 s in accordance with the changes of the temperature law $T_w(0,t)$, two time moments $t = 22.065$ s

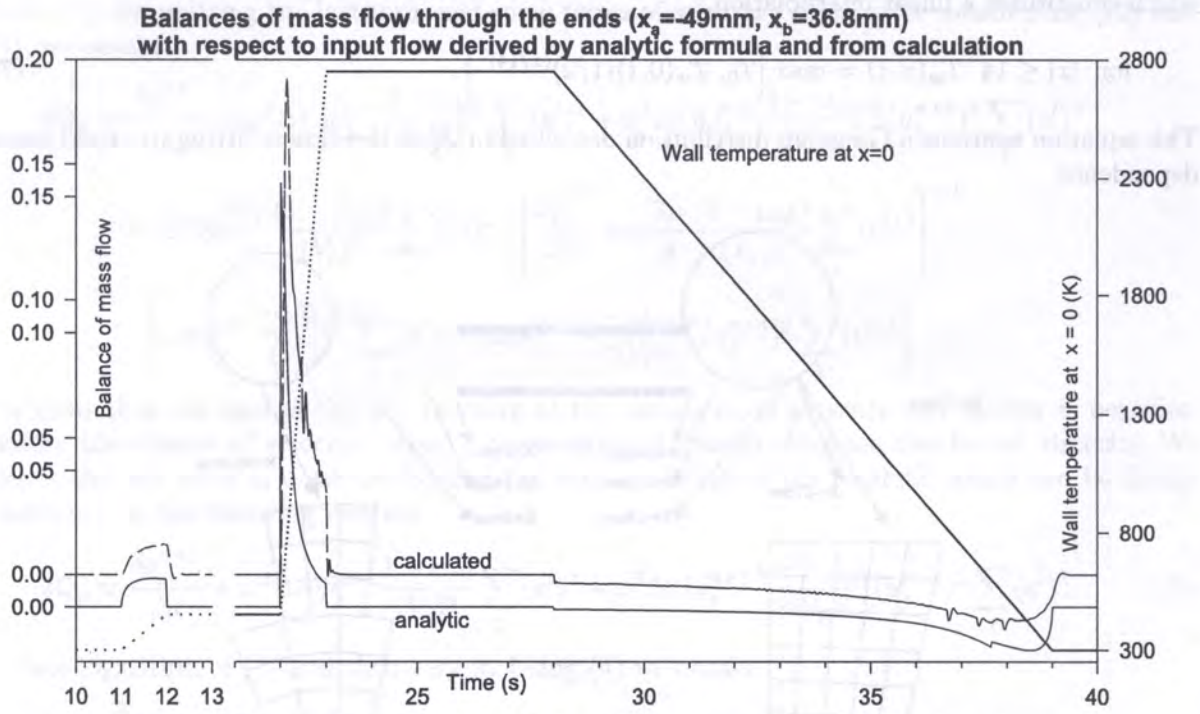

Fig. 8. Balances of mass flow through the ends for given wall temperature dependence

and 37.653 s exist where $T_w(0,t)$ is equal to 600 K; at these moments, in accordance with (74), for $x \in [14, 16.8]$, the temperature law $T_w(x,t)$ also sharply changes in time. This is the reason of the sharp change of $m_{\text{bal, an}}$. In Fig. 8 one can see also the calculated value of $m_{\text{bal, cal}}$

$$m_{\text{bal, cal}} = (m_a - m_b)/m_b\,,$$

which is derived for $x_a = -49$ mm, $x_b = 36.8$ mm in accordance with the computation region shown in Fig. 7. One can see a satisfactory correlation between the analytic and computed data. For the time region between 11 s and 12 s, where the wall temperature slightly increases and, in the tube section, the temperature of gas has a time to accept the temperature of the wall, we see that the coincidence is better than that in the case of a rapid and large increase of the wall temperature with the time in the interval from 22 s to 23 s. The above difference can also be explained by a significant convection flow which transfers over the temperature along the stream direction as one can see in Fig. 10, where the pressure, velocity and temperature spatial distributions are presented for the time $t = 25$ s. For the sake of convenience we restored the full domain of longitudinal section of the tube from the calculated axial symmetry part. In Fig. 8 the mass balance $m_{\text{bal, cal}}$ has the three sharp depressions of the curve for the time between 36.6 s to 38 s. This may be explained by the change of the heating rate from the wall due to decrease of the flow velocity. The flow carries a cold gas from the inlet and this creates a greater temperature gradient between wall and gas. The decrease of the wall temperature results in a decrease of the flow velocity. As the flow velocity decreases, this results in a decrease of the temperature gradient and therefore the rate of heating by the wall drops. Such a reduction of the heating rate is superimposed on the reduction of the heating rate due to a decrease of the wall temperature. This illustrates a physical instability of the process. The decrease of the heating rate generates a decrease of the flow velocity and *vice versa*. Certainly, the input flow produces pressure and this restricts the development of instability.

Time dependencies of the quantities which characterize the effectiveness of the numerical Newton-type global and inner pressure correction iteration procedure are given in Fig. 9. Let N be the number of calculation step at the time t, n_L be the number of global iterations at step N (time t). Assume that N_L is the general number of global iterations n_L at the step N, n_{Lp} is the number of all inner

iterations at the step N; n_{Lp} is equal to the sum of the inner iterations at every global iteration $L = 1, 2, \ldots n_L - 1$. Since at the last global iteration $L = n_L$ inner pressure correction iterations are absent, we have that $n_{Lp}/(n_L - 1)$ is the number of the inner pressure correction iterations that fall at one global iteration. In Fig. 9 the data are given at the time t changing from 0 to 50s through every $\Delta t_{\text{print}} = 0.01$ s. The quantity $\mathrm{d}N_L/\mathrm{d}N = \Delta N_L/\Delta N$ is the averaged by time Δt_{print} number of global iterations which fall at one step, where $\Delta N_L = N_L(t_{\text{print}}) - N_L(t_{\text{print}} - \Delta t_{\text{print}})$, $\Delta N = N(t_{\text{print}}) - N(t_{\text{print}} - \Delta t_{\text{print}})$. The quantity $\overline{n_{Lp}/(n_L - 1)}$ is the averaged by Δt_{print} number of inner pressure correction iterations which fall at one global iterations. Both these quantities $\mathrm{d}N_L/\mathrm{d}N$ and $\overline{n_{Lp}/(n_L - 1)}$ are restricted by 2 from below; moreover, the last one is restricted by 5 from above. As one can see, for the most part $\mathrm{d}N_L/\mathrm{d}N$ is equal to 4 or oscillates between 4 and 2 approximately, $\overline{n_{Lp}/(n_L - 1)}$ exceeds 4. The quantities $\mathrm{d}t_{\text{cal}}/\mathrm{d}t = \Delta t_{\text{cal}}/\Delta t_{\text{print}}$ and $\mathrm{d}N_L/\mathrm{d}t = \Delta N_L/\Delta t_{\text{print}}$ are the derivatives of the computation time and number of global iterations, respectively, with respect to the real time of process. Here we have $\Delta t_{\text{cal}} = t_{\text{cal}}(t_{\text{print}}) - t_{\text{cal}}(t_{\text{print}} - \Delta t_{\text{print}})$. The calculations were carried out on PC PentiumII-333. The following correlation takes place

$$\frac{\mathrm{d}t_{\text{cal}}}{\mathrm{d}t} \approx \text{const}\,\frac{\mathrm{d}N_L}{\mathrm{d}t}\left[1 + 0.1\overline{n_{Lp}/(n_L - 1)}\right],$$

where const depends on the computer performance. The areas under the curves $\mathrm{d}t_{\text{cal}}/\mathrm{d}t$ and $\mathrm{d}N_L/\mathrm{d}t$ give the computation time t_{cal} and number of global iterations N_L, respectively. After dividing the number of global iterations by $\mathrm{d}N_L/\mathrm{d}N$, we obtain the number of calculation steps N. By dividing t by N we obtain the average time step. As one can see in Fig. 8 that, as soon as the wall temperature stops to change, the stabilization time does not exceed 0.3 s. Therefore, by Fig. 9, a stabilization here requires approximately $0.3(6000 \div 8000) \approx 2000$ global iterations at $T = 300$ K, 3000 global iterations at $T = 450$ K, and 11000 global iterations at $T = 2750$ K. The corresponding numbers of computation steps are approximately 500 at $T = 300$ K, 750 at $T = 450$ K, and 3000 at $T = 300$ K. If we consider only the stationary state, then we may take the weight of scheme $\omega = 1$ instead of 0.6 to accelerate the convergence.

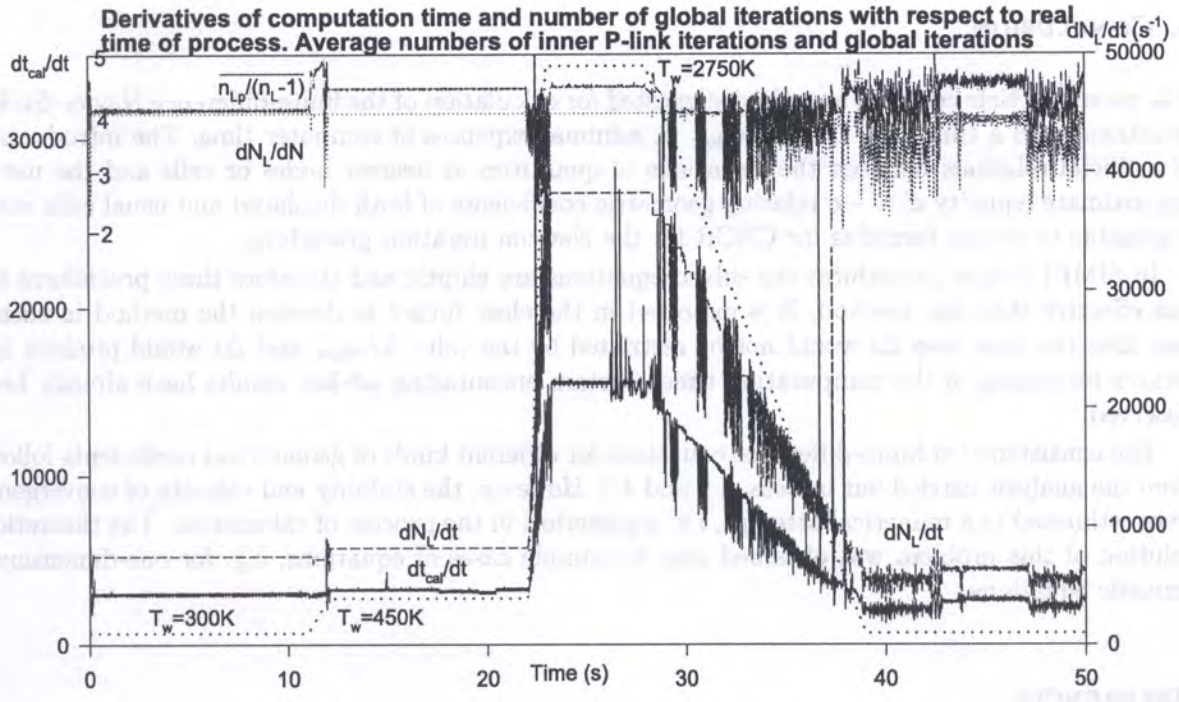

Fig. 9. Time dependence of the quantities which characterize the effectiveness of numerical Newton-type global and inner pressure correction iteration procedure for given wall temperature dependence

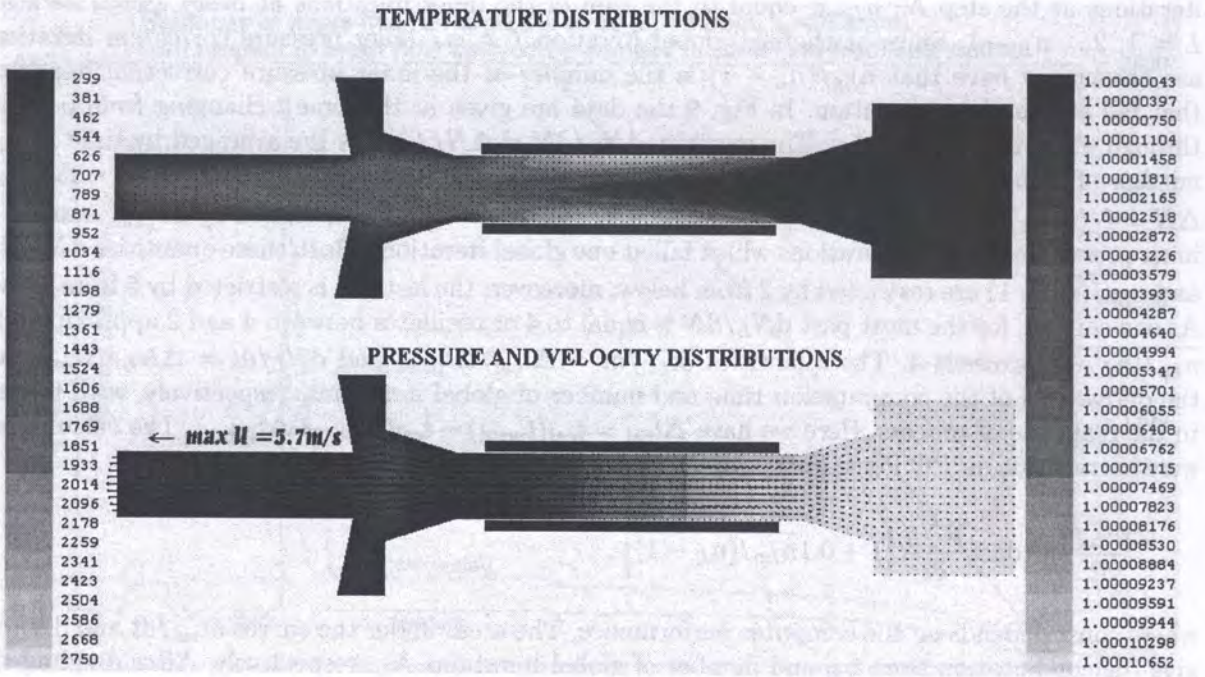

Fig. 10. The pressure, velocity and temperature spatial distributions at time $t = 25$ s

After computational experiments it turns out that, indeed, the time step Δt is approximately equal to the value h/u_{flow}. If the wall temperature increases from 300 K to 2750 K, the maximal velocity increases approximately 5.5 times but not 9 times in view of the large convection flow trasnferring over the temperature along the stream. In addition, the time step decreases approximately 5.5 times.

9. Conclusion

The present article contains a method suggested for calculation of the finite-difference Navier–Stokes equations with a time step $\Delta t = h/u_{\text{flow}}$ at minimal expenses of computer time. The introduction of artificial relations between the variations of quantities at nearest nodes or cells and the use of approximate equality $\mathbf{c}' \approx -\mathbf{c}$ relating geometric coefficients of both displaced and usual cells make it possible to obtain formulas for CRCR for the Newton iteration procedure.

In SIMPLE-type procedures the solved equations are elliptic and therefore these procedures are less effective than our method. It is expected in the close future to develop the method in such a way that the time step Δt would not be restricted by the value h/u_{flow} and Δt would produce less serious increasing of the computation time. Certain encouraging ad-hoc results have already been observed.

The consistency of finite-difference equations for different kinds of geometrical coefficients follows from the analysis carried out in Secs. 4.2 and 4.3. However, the stability and velocity of convergence were estimated in a numerical attempt, i.e. a posteriori in the process of calculation. The theoretical solution of this problem was obtained only for simple cases of equations, e.g. for one-dimensional acoustic equations.

References

[1] J.L. Ferziger, M. Peric. Computational Methods for Fluid Dynamics. Springer, 1999.

[2] S.F. Araslanov, A.Kh. Gilmutdinov, M. Sperling. 3D Numerical Simulation of the Gas Flows in Transversely Heated Graphite Tube Atomizers (CD – proceedings of European Congress on Computational Methods in Applied Sciences and Engineering ECCOMAS 2000, Barcelona, 11-14 September 2000).
[3] P.J. O'Rourke, F.V. Bracco. Two scaling transformations for the numerical computation of multidimensional unsteady laminar flames. *J. Comput. Phys.*, **33**: 185–203, 1979.
[4] W.E. Pracht, Calculating three-dimensional fluid flow at all speeds with an Eulerian-Lagrangian computing mesh. *J. Comp. Phys.*, **17**: 132–159, 1975.
[5] E.S. Oran, J.P. Boris. *Numerical Simulation of Reactive Flow.* Elsevier Science Publishing Co., 1987.
[6] J.U. Brackbill, in: Methods in Computational Physics. **16**, 11–50, Academic press, New York 1976.
[7] J. Venable, T.Williamson, J.A. Holcombe. Characterization of pressure pulse and carrier gas flow changes resulting from pulsed heating in ETV-ICP-MS. *Journ. Anal. At. Spectrom.*, **15**: 1329–1334, 2000.
[8] A.Kh. Gilmutdinov, I.S. Fishman. The theory of sample transfer in semi-enclosed atomizers for atomic absorption spectroscopy. *Spectrochim. Acta*, **39B**: 171–192, 1984.